

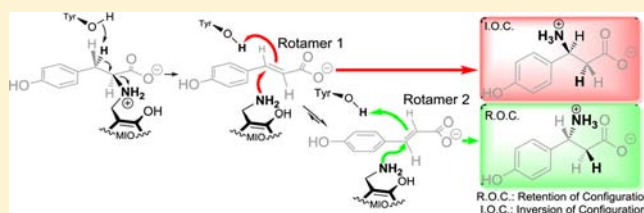
# A Bacterial Tyrosine Aminomutase Proceeds through Retention or Inversion of Stereochemistry To Catalyze Its Isomerization Reaction

Udayanga Wanninayake<sup>†</sup> and Kevin D. Walker<sup>†,‡,\*</sup>

<sup>†</sup>Department of Chemistry, and <sup>‡</sup>Department of Biochemistry and Molecular Biology, Michigan State University, East Lansing, Michigan 48824, United States

**S** Supporting Information

**ABSTRACT:**  $\beta$ -Amino acids are biologically active compounds of interest in medicinal chemistry. A class I lyase-like family of aminomutases isomerizes (*S*)- $\alpha$ -arylalanines to the corresponding  $\beta$ -amino acids by exchange of the  $\text{NH}_2/\text{H}$  pair. This family uses a 3,5-dihydro-5-methylidene-4*H*-imidazol-4-one (MIO) group within the active site to initiate the reaction. The absolute stereochemistry of the product is known for an MIO-dependent tyrosine aminomutase from *Chondromyces crocatus* (CcTAM) that isomerizes (*S*)- $\alpha$ -tyrosine to (*R*)- $\beta$ -tyrosine. To evaluate the cryptic stereochemistry of the CcTAM mechanism, (2*S*,3*S*)-[2,3-<sup>2</sup>H<sub>2</sub>]- and (2*S*,3*R*)-[3-<sup>2</sup>H]- $\alpha$ -tyrosine were stereoselectively synthesized from unlabeled (or [<sup>2</sup>H]-labeled) (4'-hydroxyphenyl)acrylic acids by reduction with D<sub>2</sub> (or H<sub>2</sub>) gas and a chiral Rh-Prophos catalyst. GC/EIMS analysis of the [<sup>2</sup>H]- $\beta$ -tyrosine biosynthesized by CcTAM revealed that the  $\alpha$ -amino group was transferred to C <sub>$\beta$</sub>  of the phenylpropanoid skeleton with retention of configuration. These labeled substrates also showed that the *pro*-(3*S*) proton exchanges with protons from the bulk media during its migration to C <sub>$\alpha$</sub>  during catalysis. <sup>1</sup>H- and <sup>2</sup>H NMR analyses of the [<sup>2</sup>H]- $\beta$ -tyrosine derived from (2*S*)-[3,3-<sup>2</sup>H<sub>2</sub>]- $\alpha$ -tyrosine by CcTAM catalysis showed that the migratory proton attached to C <sub>$\alpha$</sub>  of the product also with retention of configuration. CcTAM is stereoselective for (*R*)- $\beta$ -tyrosine (85%) yet also forms the (*S*)- $\beta$ -tyrosine enantiomer (15%) through inversion of configuration at both migration termini, as described herein. The proportion of the (*S*)- $\beta$ -isomer made by CcTAM during steady state interestingly increased with solvent pH, and this effect on the proposed reaction mechanism is also discussed.



## INTRODUCTION

$\beta$ -Amino acids are emerging as an important class of compounds that are present in bioactive natural products, such as the antineoplastic pharmaceutical paclitaxel isolated from *Taxus* plants,<sup>1,2</sup> the aminopeptidase inhibitor bestatin obtained from *Streptomyces olivoreticuli*,<sup>3</sup> an antibacterial blasticidin S from *S. griseochromogenes*,<sup>4</sup> the antibiotic agent enediyne C-1027 from *S. globisporus*,<sup>5</sup> the anti-tuberculosis agent viomycin from *S. vinaceus*,<sup>6</sup> the antibiotic andrimid from *Pantoea agglomerans*, and cytotoxic agents chondramides A–D from *Chondromyces crocatus*.<sup>7</sup> In addition, single  $\beta$ -aryl- $\beta$ -alanines show anti-epileptogenesis activity.<sup>8</sup> Other  $\beta$ -aryl- $\beta$ -alanines have been used as building blocks toward the synthesis of complex bioactive molecules, including  $\beta$ -lactams,<sup>9</sup>  $\beta$ -peptides as mimics of  $\alpha$ -peptides,<sup>10,11</sup> and antimicrobial compounds.<sup>12</sup>

Several chiral synthetic strategies have been developed for variously substituted  $\beta$ -arylalanines that include tandem one-pot processes<sup>13</sup> and conjugate addition of homochiral lithium amides to  $\alpha,\beta$ -unsaturated acceptors.<sup>14</sup> The Knoevenagel condensation of benzaldehyde and malonic acid in the presence of  $\text{NH}_4\text{OAc}$  produced a series of racemic  $\beta$ -arylalanines.<sup>15</sup> By contrast, there are only a few reports on the biocatalysis of asymmetric  $\beta$ -arylalanines from the corresponding readily

available natural and nonnatural  $\alpha$ -amino acids through aminomutase catalysis.

So far, five 3,5-dihydro-5-methylidene-4*H*-imidazol-4-one (MIO)-dependent aminomutases are known to isomerize either (*S*)- $\alpha$ -phenylalanine (EncP from *S. maritimus*,<sup>16</sup> AdmH (PaPAM) from *P. agglomerans*,<sup>17,18</sup> and TcPAM from *Taxus* plants<sup>19,20</sup>), or (*S*)- $\alpha$ -tyrosine ((*S*)-1) (SgcC4 (SgTAM) from *S. globisporus*<sup>21,22</sup> and CmdF (CcTAM) from *C. crocatus*,<sup>23</sup> further described herein) to their respective  $\beta$ -amino acids. Efforts to optimize the turnover of this family of aminomutases provides a potentially alternative means toward scalable biocatalytic production of novel enantiomerically pure  $\beta$ -amino acids as synthetic building blocks in medicinal chemistry. Earlier substrate specificity studies showed that TcPAM can convert substituted aromatic and heteroaromatic  $\alpha$ -alanines to the corresponding  $\beta$ -alanines. Apparently, since TAMs require the 4'-hydroxyl group on the substrate for catalysis, their use to biosynthesize  $\beta$ -tyrosine analogues is limited.<sup>21,23</sup>

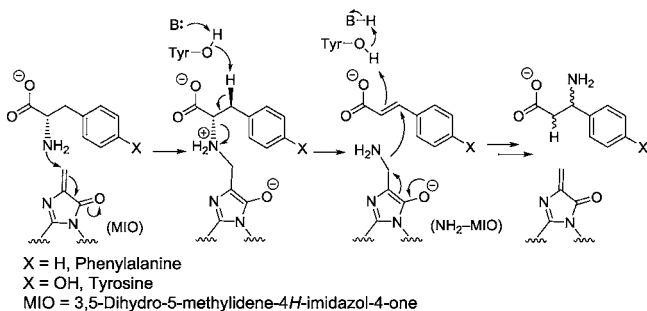
These aminomutases belong to a class I lyase-like family (comprising ammonia lyases<sup>24–26</sup> and aminomutases<sup>18,19,23,27</sup>) where, mechanistically, the amino group of the arylalanine substrate nucleophilically attacks the MIO to form an amino

Received: April 19, 2013

Published: June 25, 2013

acid–MIO adduct (Scheme 1). Removal of a  $\beta$ -proton via a tyrosine residue and concomitant elimination of the  $\text{NH}_2$ –

### Scheme 1. General MIO-Dependent Aminomutase Mechanism



MIO adduct from the substrate produces an intermediary arylacrylate product. Interchange and rebound of the transient hydrogen and  $\text{NH}_2$ –MIO to the intermediate, and release of the  $\beta$ -amino acid completes the conversion. Stereochemical evidence shows that these enzymes can be sorted by their enantioselectivity for the  $\beta$ -amino acid product; EncP, PaPAM, and SgTAM make (*S*)- $\beta$ -arylalanines, and CcTAM and TcPAM make (*R*)- $\beta$ -arylalanines. Further, the properties of the MIO aminomutases segregate according to whether the cryptic stereochemistry at  $C_\alpha$  and  $C_\beta$  of the product is inverted or retained. The different enantioselectivities of these isozymes is determined by the fate of the intermediate formed on distinct reaction pathways.

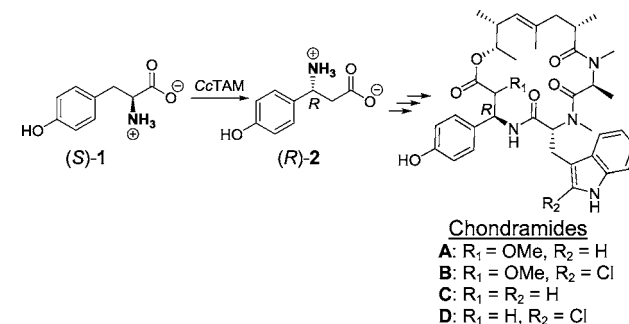
For example, both PaPAM and SgTAM presumably bind their respective substrates and displace the  $\text{NH}_2$ –MIO adduct and *pro*-(3*S*) hydrogen by *anti*-elimination. For both enzymes, the  $\text{NH}_2$ –MIO and hydrogen interchange positions and rebound to the same face of the cinnamate intermediate from which they were removed to form the (*S*)- $\beta$ -amino acids, with inversion of configuration at  $C_\alpha$  and  $C_\beta$ . Therefore, the intermediate on this reaction sequence must reside as a single rotamer.<sup>17,27</sup> By contrast, for the isozyme TcPAM, the cinnamate intermediate is proposed to rotate 180° about the  $C_1$ – $C_\alpha$  and  $C_\beta$ – $C_{\text{ipso}}$  bonds. Then the labile  $\text{NH}_2$  and *pro*-(3*S*) hydrogen exchange positions and reattach to the opposite face of the intermediate from which they were removed. This mechanism results in retention of configuration at  $C_\alpha$  and  $C_\beta$  to form (*R*)- $\beta$ -phenylalanine.<sup>17,19,28,29</sup>

Interestingly, the tyrosine aminomutases (TAMs) are less enantioselective than the PAMs. The former make both enantiomers of the  $\beta$ -tyrosine (**2**) at steady state and show significantly lower enantiomeric excess after reaching equilibrium,<sup>23,30</sup> while the PAM enzymes make product at >99% ee, even after reaching equilibrium, and racemization is not observed.<sup>17,20,28,29</sup> It should be noted that earlier mutational studies on CcTAM (Glu399 → Lys399) improved the enantioselectivity for (*R*)-**2** from 69% to 97% ee.<sup>23</sup> Despite this earlier study to correlate active site residues with the stereoselectivity of CcTAM, the reason why the  $\beta$ -amino acid enantioselectivity was enhanced remained unexplored. In addition, the mode of attachment (i.e., retention or inversion of configuration) of the reciprocally migratory  $\text{NH}_2$  group and the hydrogen at  $C_\alpha$  and  $C_\beta$  during the reaction is unknown.

To understand and ultimately improve the substrate specificity profile, turnover rate, and enantioselectivity of CcTAM, its mechanisms must be fully understood. To this

end, we add further mechanistic detail to CcTAM, which converts (*S*)-**1** to (*R*)-**2** on the biosynthetic pathway of the cytotoxic cyclodepsipeptide chondramides A–D in *C. crocatus* myxobacteria (Scheme 2).<sup>7,23,31</sup> The (*R*)-product stereo-

### Scheme 2. CcTAM Reaction on the Chondramides A–D Pathway



chemistry catalyzed by CcTAM suggested that its stereochemical course is related to that catalyzed by TcPAM. Herein, we used deuterium-labeled isotopomers of  $\alpha$ -tyrosine to evaluate the cryptic stereochemistry of the CcTAM mechanism and compare it to that of other aminomutases.

## RESULTS

**CcTAM Activity and Stereochemistry.** CcTAM was expressed from the pET-28a(+) vector in *Escherichia coli* (BL21), and then CcTAM and (*S*)-**1** were incubated. The amino acids and hydroxycinnamate were derivatized and analyzed by GC/EIMS to show that product **2** (90 mol %) and byproduct 4'-hydroxycinnamate (10 mol %) were formed. The biosynthetic  $\beta$ -tyrosine was also derivatized with a chiral auxiliary that indicated a mixture containing (*R*)-**2** and (*S*)-**2** at an 85:15 ratio (See Figures S1 and S2 in Supporting Information [SI]). This product distribution was consistent with that shown in an earlier study.<sup>23</sup>

**Assignment of the Prochiral Hydrogens of (*R*)-**2** by <sup>1</sup>H NMR.** The <sup>1</sup>H NMR of authentic unlabeled (*R*)-**2** showed signals at  $\delta$  4.41 (dd,  $J = 4.4, 10.1$  Hz,  $C_\beta$ -H), 2.73 (dd,  $J = 10.1, 16.6$  Hz,  $C_\alpha$ -H), 2.61 (dd,  $J = 4.4, 16.7$  Hz,  $C_\alpha$ -H) in CD<sub>3</sub>OD solvent (Figure 1). According to the Karplus equation for <sup>1</sup>H NMR,<sup>32</sup> <sup>3</sup> $J$  coupling constants of vicinal protons are largest when the dihedral torsion angle ( $\phi$ ) is constrained at 0° (eclipsed conformation) or 180° (*anti* conformation). Smaller <sup>3</sup> $J$  coupling constants are observed when  $\phi$  approaches 90°. Thus, the magnitudes of the <sup>3</sup> $J$  couplings ( $J_{\text{eq-eq}}$  and  $J_{\text{eq-ax}}$  ( $\phi =$

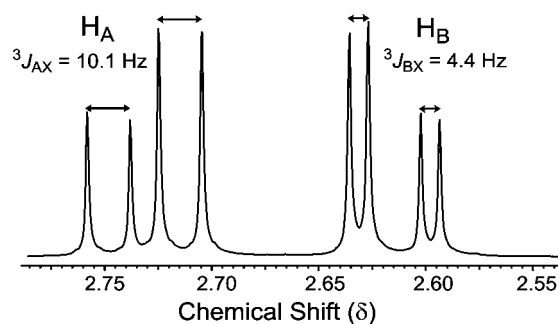


**Figure 1.** Partial <sup>1</sup>H NMR profile of unlabeled **2** and the <sup>3</sup> $J$  coupling constants for the ABX spin system of (*R*)-**2**.

60°) between 3 and 4 Hz, and  $J_{ax-ax}$  ( $\phi = 180^\circ$ ) between 8 and 13 Hz) of the conformationally restricted vicinal axial (ax) and equatorial (eq) protons of cyclohexane<sup>33,34</sup> were used as a guide to assign the  $^1\text{H}$  NMR signals of (*R*)-**2**. The geminal  $C_\alpha$ -H signals (designated as A and B spins) of the unlabeled (*R*)-**2** spin-coupled with  $C_\beta$ -H (designated as the X spin) were identified by their distinct  $J$ -values [ $AX$  ( $^3J_{AX} = 10.1$  Hz,  $\phi \approx 180^\circ$ ) and  $BX$  ( $^3J_{BX} = 4.4$  Hz,  $\phi \approx 60^\circ$ )] (Figure 1).

**Using NMR to Assess the Mechanism of the Hydrogen Transfer at  $C_\alpha$  in the CcTAM Reaction.** The  $^2\text{H}$  NMR chemical shifts of the propanoid side chain deuteriums at  $C_\alpha$  and  $C_\beta$  of [ $^2\text{H}_2$ ]-**2** biosynthesized from (*2S*)-[ $3,3\text{-}^2\text{H}_2$ ]-**1** by CcTAM were at  $\delta$  2.61 (relative peak area = 0.7) and 4.41 (relative peak area = 1.0), respectively (Figure 2A). The

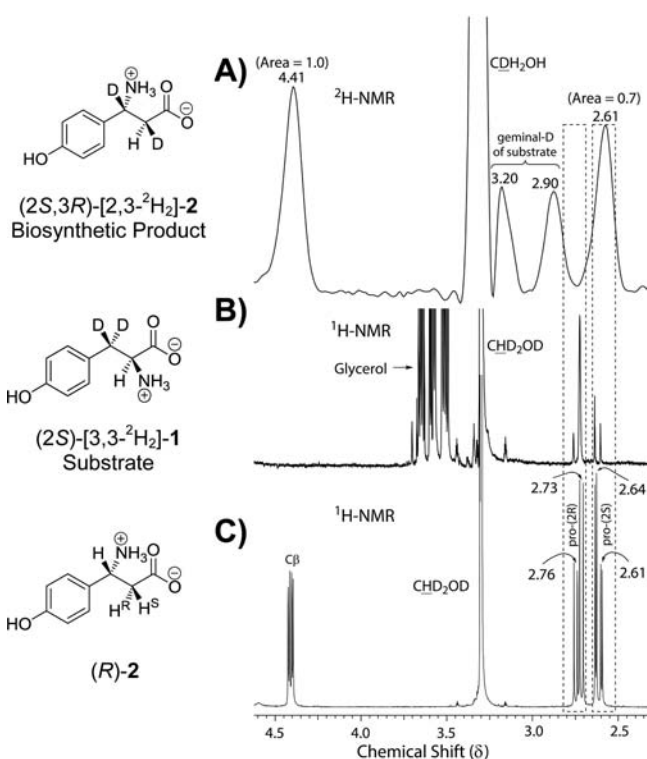


**Figure 2.**  $^2\text{H}$  NMR (after solvent exchange into  $\text{CH}_3\text{OH}$ ); the relative area of the peaks at  $\delta$  4.41 and 2.61 are shown (A) and  $^1\text{H}$  NMR (after solvent exchange into  $\text{CD}_3\text{OD}$ ) (B) of a mixture containing the remaining substrate (*2S*)-[ $3,3\text{-}^2\text{H}_2$ ]-**1** and the biosynthetic (*2S*,3*R*)-[ $2,3\text{-}^2\text{H}_2$ ]-**2** after a CcTAM-catalyzed reaction.  $^1\text{H}$  NMR (in  $\text{CD}_3\text{OD}$ ) of authentic (*R*)-**2** (C). The signals for the prochiral protons of authentic (*R*)-**2** are aligned (boxes) with signals for the deuterium labeled product in the biosynthetic sample.

deuterium signals were compared to the  $^1\text{H}$  NMR chemical shifts of the prochiral hydrogens of authentic (*R*)-**2** (Figure 2A,C) to assign the absolute stereochemistry of the [ $^2\text{H}$ ]-labeled biosynthetic sample. The  $^1\text{H}$  NMR signal at  $\delta$  2.73 (singlet) produced by the biosynthetic [ $^2\text{H}$ ]-labeled (*R*)-**2** (Figure 2B) coincided with the chemical shift of the *pro*-(2*R*) proton of authentic (*R*)-**2** (Figure 2C). Two nearby doublets were also observed at  $\delta$  2.75 (d,  $J = 16.8$  Hz, 1 H) and 2.63 (d,  $J = 16.8$  Hz, 1 H) with a peak area that was  $\sim 30\%$  of the singlet at  $\delta$  2.73 (Figure 2B). These resonances corresponded to a [ $^2\text{H}$ ]-labeled isotopomer of **2** containing two geminal hydrogens at  $C_\alpha$  creating an AB-coupled spin system.

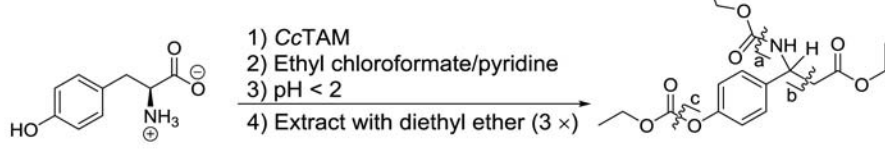
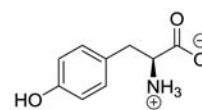
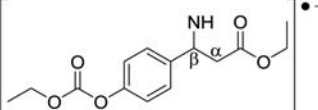
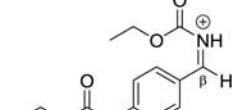
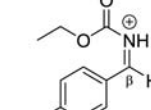
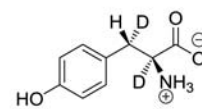
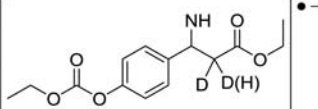
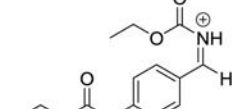
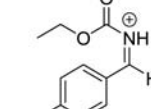
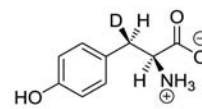
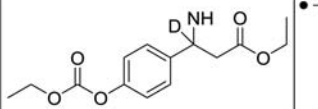
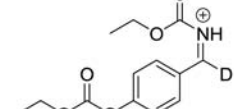
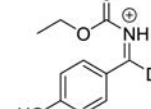
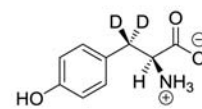
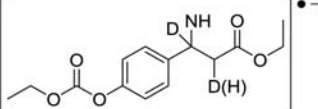
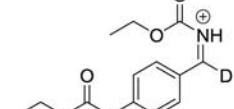
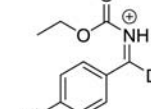
**Assessing the Mode of the Amino Group Attachment at  $C_\beta$  by CcTAM.** Synthesis of (*2S*,3*S*)-[ $2,3\text{-}^2\text{H}_2$ ]- and (*2S*,3*R*)-[ $3\text{-}^2\text{H}$ ]-**1**. The mode of the amino group transfer to  $C_\beta$  during the isomerization reaction catalyzed by CcTAM was assessed. (*2S*,3*S*)-[ $2,3\text{-}^2\text{H}_2$ ]- and (*2S*,3*R*)-[ $3\text{-}^2\text{H}$ ]-**1** were synthesized by stereospecific reduction of unlabeled and [ $3\text{-}^2\text{H}$ ]-labeled (*Z*)-2-benzamido-3-(4'-hydroxyphenyl)acrylic acid using a chiral  $[\text{Rh}((\text{R})\text{-Prophos})(\text{NBD})]\text{ClO}_4$  catalyst with deuterium or hydrogen gas, according to an earlier procedure.<sup>35</sup> The [ $^2\text{H}$ ]-labeled isotopomers of **1** were treated with a chiral auxiliary (*S*)-2-methylbutyric anhydride and titrated with diazomethane to make the 4'-*O*,3-*N*-di((*S*)-2-methylbutanoyl)- $\alpha$ -tyrosine methyl ester derivatives. The retention times and mass spectrometry fragmentation of the synthesized [ $^2\text{H}$ ]-labeled (*S*)-**1** derivatives observed by GC/EIMS analysis were identical to those of an identically derivatized sample of authentic (*S*)-**1**.

**Analysis of **2** Made by CcTAM Catalysis from (*2S*,3*S*)-[ $2,3\text{-}^2\text{H}_2$ ]- and (*2S*,3*R*)-[ $3\text{-}^2\text{H}$ ]-**1**.** CcTAM was incubated separately with (*2S*,3*S*)-[ $2,3\text{-}^2\text{H}_2$ ]- and (*2S*,3*R*)-[ $3\text{-}^2\text{H}$ ]-**1**. Afterward, the reaction was basified, and the amino acids were derivatized to their 4'-*O*,3-*N*-di(ethoxycarbonyl) derivatives, acidified, extracted from the aqueous reaction buffer, and reacted with diazomethane to make the methyl esters. Interestingly, during the basification step of the derivatization procedure, ethanol byproduct from the excess ethyl chloroformate caused partial ethyl esterification of the amino acids (10–30 mol % compared to the methyl esters). The mass spectrum of the methyl ester derivatives of the  $\beta$ -isomers yielded ions of diagnostic labeled fragments that were perturbed by overlapping satellite fragment ions. Therefore, the ethyl esters of the  $\beta$ -isomers were separated by GC, and the fates of the deuteriums on the  $\beta$ -amino acids, originating from the substrate, were evaluated by the identity of diagnostic fragment ions made in the mass spectrometer (see SI Figures S3–S5 for fragment ions). The molecular ion [ $\text{M}^+$ ] ( $m/z$  353) of the 4'-*O*,3-*N*-di(ethoxycarbonyl) ethyl ester derivative of unlabeled (*R*)-**2** fragmented into diagnostic ions **F1A**, **F2A**, and **F3A** ( $m/z$  280, 266, and 194, respectively) (Table 1A). The corresponding fragment ions of the derivatized  $\beta$ -amino acid biosynthesized by CcTAM from (*2S*,3*S*)-[ $2,3\text{-}^2\text{H}_2$ ]-**1** were **F1B**, **F2B**, and **F3B** ( $m/z$  282, 266, and 194, respectively, Table 1B). Fragment ions **F2B** ( $m/z$  266) and **F3B** ( $m/z$  194) are identical to those of the unlabeled derivatized product (Table 1A), indicating that deuterium was not at  $C_\beta$  of the biosynthetic **2**. Further, the fragment ion **F1B** ( $m/z$  282, Table 1B) corresponding to the intact phenylpropanoid was shifted by two mass units above the similar fragment ion of the unlabeled isotopomer. These data indicate that both deuteriums are at  $C_\alpha$  of the biosynthetic product derived from (*2S*,3*S*)-[ $2,3\text{-}^2\text{H}_2$ ]-**1**. Notably, the mass spectrum of the biosynthetic product **2** made from (*2S*,3*S*)-[ $2,3\text{-}^2\text{H}_2$ ]-**1** showed a molecular ion ( $[\text{M}^+]$ ,  $m/z$  355) and ion  $m/z$  354 ( $[\text{M}^+]$ ), one mass unit lower (Table 1B), indicating 36% deuterium was lost from the product compared to the substrate. This deuterium-to-hydrogen (D  $\rightarrow$  H) exchange during the CcTAM isomerization of (*2S*,3*S*)-[ $2,3\text{-}^2\text{H}_2$ ]-**1** was also supported by the ratio of diagnostic fragment ion **F1B** ( $m/z$  282) (Table 1B) and its [**F1B** - 1] partner ( $m/z$  281), showing 32% deuterium loss.

Conversely, when (*2S*,3*R*)-[ $3\text{-}^2\text{H}$ ]-**1** was used as the substrate with CcTAM, the resulting derivatized [ $^2\text{H}$ ]-labeled **2** yielded fragment ion **F1C** ( $m/z$  281) that was shifted one mass unit over its unlabeled counterpart (Table 1C), indicating retention



Table 1. EI-MS Fragmentation of 4'-O,3-N-Di(ethoxycarbonyl) Ethyl Ester Derivatives of Labeled and [ $^2\text{H}$ ]-Labeled Biosynthesized Isotopomers of **2**

				
Isotopomers of Substrate <b>1</b>	Fragment ion F1: Cleavage at bond a	Fragment ion F2: Cleavage at bonds b	Fragment ion F3: Cleavage at bonds b, c; H-transfer <sup>d</sup> to O	
<b>A) (2S)-unlabeled</b> 	 <i>m/z</i> 280	 <i>m/z</i> 266	 <i>m/z</i> 194	
<b>B) (2S,3S)-[2,3-<math>^2\text{H}_2</math>]</b> 	 <i>m/z</i> 282 ( <i>m/z</i> 281 D→H exchange)	 <i>m/z</i> 266	 <i>m/z</i> 194	
<b>C) (2S,3R)-[3-<math>^2\text{H}</math>]</b> 	 <i>m/z</i> 281	 <i>m/z</i> 267	 <i>m/z</i> 195	
<b>D) (2S)-[3,3-<math>^2\text{H}_2</math>]</b> 	 <i>m/z</i> 282 ( <i>m/z</i> 281 D→H exchange)	 <i>m/z</i> 267	 <i>m/z</i> 195	

<sup>d</sup>D-transfer was negligible compared to H-transfer based on analysis of mass spectrometry fragments.

of one deuterium in the propanoid side chain. Fragment ions F2C (*m/z* 267) and F3C (*m/z* 195) (Table 1C) were also one mass unit higher than the corresponding fragments derived from the unlabeled product. The latter clarified that the deuterium at  $C_\beta$  of the substrate remained at this position after the CcTAM isomerization reaction to **2**.

**Assessing the D → H Exchange Rate during CcTAM Catalysis.** (2S)-[3,3- $^2\text{H}_2$ ]-**1** was incubated with CcTAM in a time course experiment to assess the extent of the D → H exchange during the isomerization (Table 1D). The  $\beta$ -amino acids isolated at designated time intervals were derivatized, and their 4'-O,3-N-di(ethoxycarbonyl) ethyl esters were analyzed by GC/EIMS, as before. Tracking the molecular ion [ $^2\text{H}_2$ ](M)<sup>+</sup> (*m/z* 355) and its [ $^2\text{H}_1$ ](M)<sup>+</sup> partner (*m/z* 354) showed that the deuterium enrichment decreased from 85% at 10 min to 60% after 12 h, under steady-state reaction conditions. After 45 h, the reaction reached equilibrium (70% conversion of substrate to products 4'-hydroxycinnamate and **2**, and the D → H exchange stabilized at 30% deuterium retention (see Table 1D and SI Figure S6–S8). Moreover, the relative abundances of fragment ions F2D (*m/z* 267) and F3D (*m/z* 195) (Table 1D) (both one mass unit above their unlabeled counterparts) from the derivatized biosynthetic product **2**, at each time point, confirmed that a deuterium remained at  $C_\beta$ .

Thus, one of the geminal deuteriums of (2S)-[3,3- $^2\text{H}_2$ ]-**1** was 100% retained at  $C_\beta$  of the product, while the migratory deuterium was partially exchanged with hydrogen. This deuterium loss during the reaction was supported by the parallel decrease in the ratio between ion F1D (*m/z* 282) (a fragment containing two deuteriums, one at  $C_\alpha$  (exchanged during catalysis), the other at  $C_\beta$  (100% retained)) and ion [F1D – 1] (*m/z* 281) (a fragment containing one deuterium at  $C_\beta$ ) in the same spectrum (Table 1D and see Figure S6 in SI as reference).

**Re-evaluation of the Stereoisomeric Product Distribution Catalyzed by CcTAM.** A previous study on CcTAM reported that the enzyme stereoselectivity was 69% ee for (*R*)-**2** at pH 8.8.<sup>23</sup> The earlier study, however, also showed that (*S*)-**2** was produced at <5 mol % for the duration of the steady state (0–4 h) of the reaction containing CcTAM (10–50  $\mu\text{g}$ ) but increased significantly as the reaction entered equilibrium.<sup>23</sup> This interesting perturbation in the production of (*R*)- and (*S*)-**2** at equilibrium prompted us to re-evaluate this reaction phenomenon. Here, GC/EIMS was used to separate the diastereoisomeric 4'-O,3-N-di((*S*)-2-methylbutanoyl)- $\beta$ -tyrosine methyl ester derivatives of the enantiomers of **2** produced by CcTAM at steady state. Even after 1% conversion of the substrate, after 5 min, CcTAM (50  $\mu\text{g}$ ) was already producing

an enantiomeric mixture containing 80% ee of (*R*)-**2** from 1 mM of substrate. The mixture approached 85:15 *R/S* (i.e., 70% ee of (*R*)-**2**) at a steady-state rate just before reaching equilibrium at 120 min (Figure 3 and Figure S2 of the

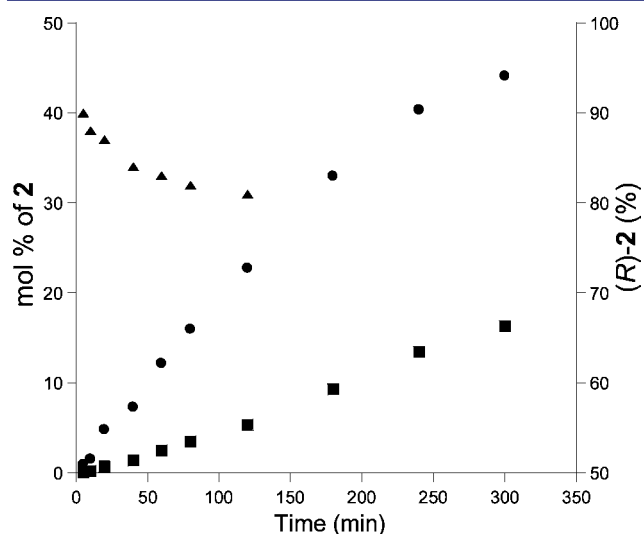


**Figure 3.** Analysis of the diastereomeric mixture of products catalyzed by CcTAM. Plotted are mol % of (*R*)-**2** (●) and (*S*)-**2** (■) relative to amount of (*S*)-**1** added. The amount of (*R*)-**2** (as %) (▲) relative to the total amount of (*R*)- and (*S*)-**2** made at steady state. (Average of duplicate assays is plotted).

Supporting Information). The steady-state production of (*S*)-**2** (from 5 to 15 mol %) over 2 h starkly contrasted the <5 mol % production of (*S*)-**2** prior to reaching equilibrium over 4 h, as reported earlier.<sup>23</sup>

**pH Effect on the Stereoselectivity of the Reaction Catalyzed by CcTAM.** The CcTAM reaction was incubated with (*S*)-**1** separately at different pH values. After the conversion of (*S*)-**1** to **2** reached 13, 35, and 56% at each pH, the amount of the (*S*)-isomer (the minor antipode) relative to the total amount of **2** was calculated. The rate of the reaction was similar at pHs 8 and 9, yet half as fast at pH 7. After the conversion of substrate to product reached ~13% in each assay, the samples incubated at pHs 7, 8, and 9 contained respectively 10.8%, 13.0%, and 16.7% (*S*)-**2**, relative to the (*R*)-antipode (Figure 4). At higher percentages of conversion, the proportion of (*S*)-**2** continued to increase, and the trend of increasing production of (*S*)-**2** with higher pH was also maintained (Figure 4).

## DISCUSSION

**Retention of Configuration at the Migration Termini during the CcTAM Reaction. Amino Group Migration.** The stereochemistry of the major biosynthetic product **2** made by CcTAM was confirmed herein as (*3R*); this was consistent with the assignment made in an earlier report.<sup>23</sup> The synthesis of stereospecifically deuterium-labeled isotopomers (*2S,3S*)-[2,3-<sup>2</sup>H<sub>2</sub>]-**1** and (*2S,3R*)-[3-<sup>2</sup>H]-**1** made it possible to assess the mode of attachment of the amino group at C<sub>β</sub> during the isomerization reaction catalyzed by CcTAM. GC/EIMS profiles of derivatized isotopomers of **2** showed diagnostic fragment ions that informed on the location of the deuteriums. Fragment ions **F2B** and **F3B** (Table 1B) revealed that the C<sub>β</sub> deuterium

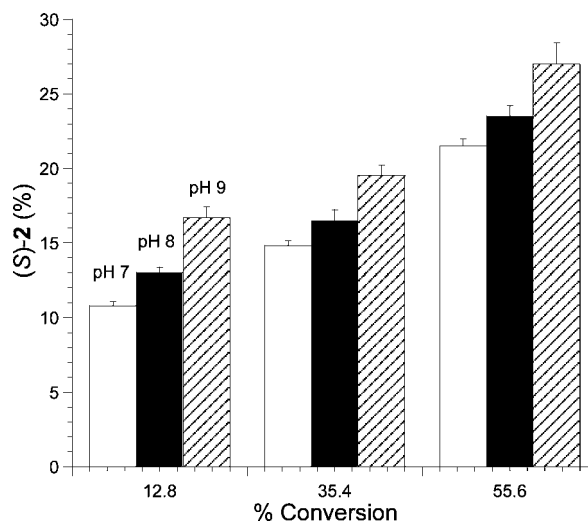


**Figure 4.** (*S*)-**2** (as % of total **2**) measured after substrate (*S*)-**1** was depleted by 13%, 35%, and 56% at pH 7, 8, and 9 while incubated with CcTAM.

of the (*2S,3S*)-[2,3-<sup>2</sup>H<sub>2</sub>]-**1** substrate was replaced by the amino group en route to **2** (Table 1).

Fragment ion **F1B** revealed that the deuterium migrated reciprocally to C<sub>α</sub> (Table 1B), thus confirming that CcTAM migrated the *pro*-(*3S*) hydrogen from C<sub>β</sub> to C<sub>α</sub>. Further, fragments ions **F2C** and **F3C** of the derivatized [<sup>2</sup>H]-labeled product (Table 1C) showed complementary that the C<sub>β</sub> deuterium of the (*2S,3R*)-[3-<sup>2</sup>H]-substrate was retained at its original position. Coupled with the known (*R*)-**2** stereochemistry made in the aminomutase reaction, the deuterium remaining at C<sub>β</sub> confirmed that CcTAM uses a retention-of-configuration mechanism at the amino migration terminus.

**Hydrogen Migration Stereochemistry.** The transient C<sub>β</sub>-deuterium of (*2S,3S*)-[2,3-<sup>2</sup>H<sub>2</sub>]-**1** migrates from C<sub>β</sub> to C<sub>α</sub> as the amino group moves reciprocally from C<sub>α</sub> to C<sub>β</sub>. The stereochemical mode of attachment of the deuterium to C<sub>α</sub> was assessed by <sup>1</sup>H- and <sup>2</sup>H NMR analyses of the zwitterion of the product dissolved in methanol. The magnitude of the difference between the AX and BX coupling constants ( $\Delta^3J \approx 6$  Hz) of (*R*)-**2** was measured and compared to the experimentally calculated  $\Delta^3J$  (~7 Hz) for the vicinal protons of the cyclohexane structure.<sup>33,34</sup> These similar  $\Delta^3J$  magnitudes calculated for these two structures suggested that the propionate hydrogens of (*R*)-**2** are conformationally restricted as they are in cyclohexane. It can be imagined that a monodentate interaction between the ammonium cation and carboxylate anion of the (*R*)-**2** zwitterion forms a pseudo-staggered six-membered ring to account for the magnitude of the observed  $\Delta^3J$  (Figure 5).

To support the proposed restricted rotamer conformation, the carboxylate group of (*R*)-**2** was methyl esterified to disrupt the ionic ammonium/carboxylate ionic interaction. In acyclic systems, the conformational preference of hydrogens in an ABX spin system is commonly lower than in a restricted conformer. As an example, <sup>3</sup>J<sub>(AX)</sub> (7.8 Hz) and <sup>3</sup>J<sub>(BX)</sub> (6.3 Hz) coupling constants ( $\Delta^3J_{(AX)-(BX)} = 1.5$  Hz) of the (*R*)-**2** methyl ester were nearly identical in CD<sub>3</sub>OD. This observation suggested that H<sub>A</sub> and H<sub>B</sub> in the (*R*)-**2** methyl ester was conformationally more equivalent with respect to H<sub>X</sub> due to greater rotational freedom about the C<sub>α</sub>-C<sub>β</sub> bond. This likely resulted from

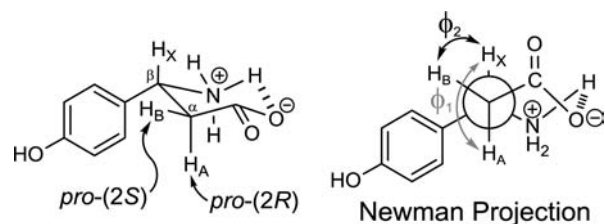


**Figure 5.** Intramolecular salt-bridge between the ammonium ion and carboxylate group of (*R*)-**2** in methanol. Dihedral angles ( $\phi_1$  and  $\phi_2$ ) between  $H_A$  and  $H_X$  and between  $H_B$  and  $H_X$ , respectively, in the pseudo-six-membered ring formed by **2** are shown in Newman Projection.

removal of the *intramolecular* ionic interaction of underivatized (*R*)-**2** (see Figure 5).

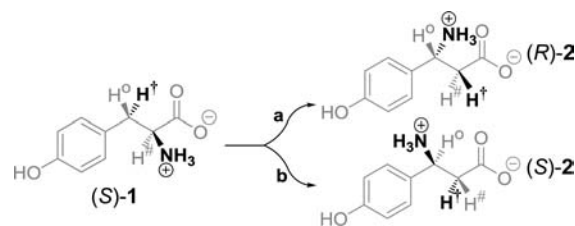
The proposed six-membered ring conformation of (*R*)-**2** places the side chain hydrogens of the amino acid in defined axial and equatorial positions by restricted rotation about the  $C_\alpha$ - $C_\beta$  bond (Figure 5). In addition, the carboxylate and aromatic ring of (*R*)-**2** are considered to be positioned *anti*, according to a described lowest energy rotamer of **1**.<sup>36</sup> Therefore, based on the  $^1\text{H}$  NMR chemical shifts and coupling constants,  $H_A$  was definitively assigned as *pro*-(2*R*) and  $H_B$  as *pro*-(2*S*) (see Figure 1). These chemical shift assignments were used as reference in  $^1\text{H}$ - and  $^2\text{H}$  NMR analyses of the deuterium-labeled biosynthetic samples. *CcTAM* shuttled one deuterium of (2*S*)-[3,3- $^2\text{H}_2$ ]-**1** from  $C_\beta$  and attached it to  $C_\alpha$  with retention of configuration, placing the deuterium in the formal *pro*-(2*S*) position of (*R*)-**2**.

Previous stereochemical studies showed that a related MIO-dependent phenylalanine aminomutase from *Taxus* plants (*TcPAM*) exchanges the position of the  $\text{NH}_2$  and hydrogen migration partners of (*S*)- $\alpha$ -phenylalanine with retention of configuration at the terminal carbons.<sup>7</sup> Thus, the *CcTAM* and *TcPAM* reactions are likely mechanistically similar,<sup>19</sup> where both remove  $\text{NH}_2$  and H from their substrates to form an acrylate intermediate. Apparently, these enzymes can rotate their intermediates 180° about the  $C_1$ - $C_\alpha$  and  $C_\beta$ - $C_{\text{ipso}}$  bonds prior to the rebound of  $\text{NH}_2$  and H to retain the stereochemistry in the corresponding  $\beta$ -products.<sup>28</sup>

It is important to note that (*R*)-**2** produced by *CcTAM* decreased from 90% to 80% (while (*S*)-**2** increased accordingly) during the steady-state phase of the reaction from 5 to 120 min (Figure 3). The isotope enrichment in fragment ion clusters of the biosynthetic [ $^2\text{H}$ ]-**2** (Table 1) in the mass spectrometer did not indicate that the (*S*)-isomer was labeled regioselectively different from (*R*)-**2**. In addition,  $^2\text{H}$  NMR analysis of the labeled mixture of **2** indicated isochronous signals for the deuteriums at  $C_\alpha$  of both enantiomers of **2** present in the reaction mixture. Therefore, the biosynthetic [ $^2\text{H}$ ]-(*S*)-**2** was labeled as the enantiomer of (*R*)- $\beta$ -isomer. In contrast to the retention-of-configuration mechanism to access (*R*)-**2**, *CcTAM* must use an inversion-of-configuration process to obtain the (*S*)-isomer (Scheme 3).

**Hydrogen Exchange during Migration.** (2*S*)-[3,3- $^2\text{H}_2$ ]-**1** was incubated with *CcTAM* in a time course study to track the  $\text{D} \rightarrow \text{H}$  exchange rate of the migratory *pro*-(3*S*) deuterium during the isomerization reaction. The deuterium enrichment in the [ $^2\text{H}$ ]-**2** decreased from 85% at 5 min to 30% after 10 h as the reaction reached equilibrium. This level of  $\text{D} \rightarrow \text{H}$  exchange was also observed for the (*R*)- $\beta$ -phenylalanine product made in a similar reaction catalyzed by the plant

### Scheme 3. Inversion and Retention of Configuration Pathways Catalyzed by *CcTAM*<sup>a</sup>



<sup>a</sup>(Path a) Retention and (Path b) inversion-of-configuration at  $C_\alpha$  and  $C_\beta$  after exchange and reattachment of the *pro*-(3*S*) proton ( $\text{H}^\dagger$ ) and the  $\text{NH}_2$  of the (*S*)-**1** substrate to make (*R*)-**2** and (*S*)-**2**, respectively by *CcTAM* catalysis.

*TcPAM* with (2*S*)-[3,3- $^2\text{H}_2$ ]- $\alpha$ -phenylalanine as the substrate.<sup>19</sup> However, no deuterium exchange was observed in the reaction catalyzed by an isozyme (*PaPAM*) from the bacteria *P. agglomerans* with (2*S*)-[3,3- $^2\text{H}_2$ ]- $\alpha$ -phenylalanine substrate.<sup>17</sup> Structural data showed that the *PaPAM* active site is slightly smaller and more ordered than *TcPAM*.<sup>28,29</sup> Thus, bulk water likely can access the active site of *TcPAM* better than that of *PaPAM*. While the *CcTAM* structure is not yet solved, it can be imagined that its active site, like that of *TcPAM*, allows access by bulk water to account for the observed proton exchange during catalysis.

The  $\text{D} \rightarrow \text{H}$  exchange rate progressively increases as the reaction progresses under steady-state conditions. A monoprotic Tyr52 residue, also reported for other MIO aminomutases (and located on a flexible loop structure),<sup>22,28,29</sup> presumably serves as the general base in the *CcTAM* reaction. In this case, after deuterium abstraction from the (2*S*)-[3,3- $^2\text{H}_2$ ]-**1**, the  $\text{D} \rightarrow \text{H}$  exchange on the catalytic Tyr52 should theoretically remain constant if all of the conditions stayed the same for the duration of the reaction; however, this is not the case. One notion to explain the observed increase in deuterium washout uses ureases as a model. Ureases are known to change the pH of the enzyme-microenvironment upon release of ammonia from urea.<sup>37,38</sup> Likewise, each of the known MIO-dependent arylalanine aminomutases catalyzes an ammonia lyase reaction that releases ammonia and produces an arylacrylate as a byproduct (see Figure S8 in SI).<sup>17,23,28,30</sup> Thus, the microenvironment of *CcTAM*, containing increasing amounts of ammonia, might increase the pH and influence the proton exchange rates during catalysis. It is conceivable that as the microenvironment ultimately reaches equilibrium with bulk water, the  $\text{D} \rightarrow \text{H}$  exchange becomes zero order as the reaction reaches equilibrium (see Figure S8 of the SI). To assess this, *CcTAM* was separated from the (2*S*)-[3,3- $^2\text{H}_2$ ]-**1** substrate and biosynthesized products after a 24-h time course study. The isolated enzyme was reincubated with more (2*S*)-[3,3- $^2\text{H}_2$ ]-**1**, and the change in the deuterium washout rate was the same as observed before (see Figure S8 in SI). Thus, the factors affecting the deuterium exchange were reversible, and the microenvironment was reset to its initial conditions.

**Diastereomeric Product Ratio Catalyzed by *CcTAM*.** Thus far, the MIO-dependent aminomutases can be categorized according to their stereoselectivity. The catalyses of *SgTAM* and *PaPAM* stereoselectively produce (*S*)- $\beta$ -arylalanines.<sup>17,18</sup> It can be imagined that these aminomutases follow a similar stereochemical course during removal and rebounding of the transient hydrogen and  $\text{NH}_2$  groups. The crystal structures of a



phenylalanine aminomutase (*PaPAM*) (Figure 6A) and a tyrosine aminomutase (*SgTAM*) (Figure 6B) show that the

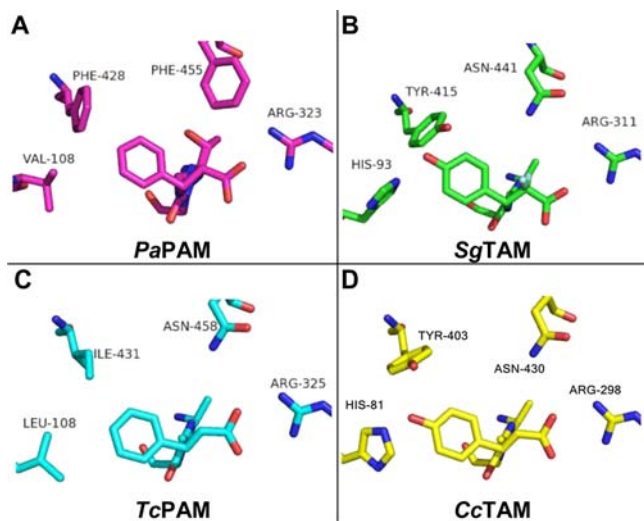


**Figure 6.** Comparison of the *TcPAM*, *PaPAM*, and *SgTAM* active-site structures cocrystallized with phenylpropanoid adducts or complexes and the *CcTAM* active site with 4'-hydroxycinnamate was modeled on the *TcPAM* crystal structure (PDB 3NZ4). The orientation of phenylpropanoid (center of each diagram) relative to the Arg residue (at the right of each diagram) is shown. Also shown are key noncatalytic residues involved in binding and positioning the substrate; the catalytic tyrosine residue is above the plane in each drawing and is not shown.

trajectories of the phenylalanine and tyrosine substrates, respectively, are nearly identical. However, these aminomutases use distinct enzyme/substrate interactions to orient their substrates. *SgTAM* apparently uses residues His93 and Tyr415 to form a hydrogen-bond network with the 4'-OH of the tyrosine substrate and place the carboxylate in a monodentate salt bridge interaction with Arg311.<sup>39</sup> By contrast, these H-bond interactions are absent in *PaPAM*, which has hydrophobic residues Val108 and Phe428 positioned analogously to His93 and Tyr415, respectively, of *SgTAM*. Instead, *PaPAM* uses the steric bulk of Phe455 to force the phenylalanine substrate into a monodentate salt bridge interaction with Arg323. This steric interaction aligns phenylalanine in *PaPAM* at an orientation similar to that of the enzyme/substrate pairing in *SgTAM*. It was postulated that, after elimination of the hydrogen and  $\text{NH}_2$  from the *PaPAM* substrate, the distinct angle somehow prevents rotation of the cinnamate intermediate. In this way, the hydrogen and  $\text{NH}_2$  can rebound to the same face of the intermediate from which they were removed. The similar substrate-docking conformations and trajectories of *PaPAM* and *SgTAM* likely, in part, define their identical (3*S*)-product stereoselectivities.

By analogy, *CcTAM* (described herein) and *TcPAM* from *Taxus* plants both make  $\beta$ -amino acid products with (3*R*)-stereochemistry;<sup>7,20,23</sup> thus, these aminomutases likely progress through similar stereochemical profiles. Earlier structural analyses showed that *TcPAM* has Asn458 positioned in contrast to the sterically larger Phe455 of isozyme *PaPAM*. The smaller Asn of *TcPAM* enables the carboxylate of the transient cinnamate intermediate to engage in a bidentate salt bridge with Arg325 (Figure 6C). In addition, the aryl portion of cinnamate sits in a hydrophobic pocket that is, in part,

composed of residues Leu108 and Ile431, which also helps align the reaction intermediate in *TcPAM*  $\sim 15^\circ$  different from that of phenylalanine about the  $C_\beta$ -axis in the *PaPAM*<sup>29</sup> (Figure 6A). The altered angle presumably allows the *TcPAM* intermediate to rotate  $180^\circ$  and retain the configuration at the chiral and prochiral centers of the (*R*)- $\beta$ -phenylalanine product. *CcTAM* probably also proceeds through an identical process to obtain (*R*)-2.

The *CcTAM* structure has not yet been solved. However, its reaction stereochemistry (retention of configuration at both  $C_\alpha$  and  $C_\beta$  in the major reaction product) is identical to that of *TcPAM*. This suggested that the two enzymes have common active-site architecture and likely position their reaction intermediates similarly. Thus, *CcTAM* was modeled on *TcPAM* (PDB 3NZ4) (30% sequence similarity). Placing the 4'-hydroxycinnamate in an orientation identical to that of cinnamate in *TcPAM* shows the hydroxyaryl portion of the former interacts with His81 and Tyr403 residues of *CcTAM* (Figure 6D). The plausible hydrogen bonding between *CcTAM* and the 4'-hydroxyaryl of the substrate likely helps align the substrate with Arg298 to form a bidentate salt bridge interaction (Figure 6D), similar to the interaction in *TcPAM*.

As mentioned, a significant difference between the aminomutase isozymes is the TAMs use His and Tyr residues in the aromatic pocket to help bind and orient the tyrosine substrate through hydrogen bonding. The PAMs, instead, use hydrophobic residues in the aromatic pocket and likely other not yet fully understood factors to direct the substrate binding orientation and stereoselectivity. It is feasible that hydrogen bonding with the phenol of the substrate, in part, governs the stereoselectivity of the TAMs and enables the minor antipodal product to form through a new reaction route. As mentioned previously, each MIO-dependent arylalanine aminomutases catalyzes an ammonia lyase reaction, releasing ammonia and an arylacrylate as byproducts (see Figure S8 in SI).<sup>17,23,28,30</sup> We posited earlier that the observed  $\text{D} \rightarrow \text{H}$  exchange for the *CcTAM* reaction was likely influenced by the increased pH of the microenvironment caused by ammonia release (Figure S8 in SI). Variation in bulk and local pH is known generally to disturb H-bonding networks within an enzyme active site.<sup>40–42</sup> In the TAM enzymes, the perturbation of the local pH could also affect the H-bonding network within the active site. Alteration of the H-bonding network in the 4'-hydroxyaryl binding pocket of the TAM enzymes could potentially change the enantioselectivity, since this region likely contributes significantly to the substrate docking conformation. Therefore, in this study, the buffered pH of a *CcTAM* reaction was adjusted to 9 and below to assess whether this would change the % ee of the product.

A lower % conversion of (*S*)-1 to 2 correlated with a higher % ee of (*R*)-2 for each pH tested. Also, at higher pH, the relative proportion of (*S*)-2 made by *CcTAM* increased compared to that of (*R*)-2. *CcTAM* consistently produced more (*S*)-2 enantiomer at higher pH, regardless of the amount of (*S*)-1 converted to 2 (Figure 4). As we proposed earlier, (*S*)-2 is made via a conformer of a 4'-hydroxycinnamate intermediate that receives the  $\text{NH}_2$  group and hydrogen (dwelling temporarily on the enzyme) on the same face from which they were removed (*S*)-1. (*R*)-2 is provided via a rotamer of the initially formed conformer of 4'-hydroxycinnamate. Therefore, since the production of (*S*)-2 increases with higher pH, these conditions can be imagined to restrict the rotation of the 4'-hydroxycinnamate intermediate within the *CcTAM*

active site by possibly altering the substrate binding angle or by strengthening the H-bond network with the 4'-OH of the substrate. Increases in pH are known to partition the phenol groups of active-site tyrosines to the phenolates and thereby shorten H-bond distances interacting with these oxyanions.<sup>41</sup> However, the mechanism through which the pH exactly affects the product stereochemistry of CcTAM remains unclear and will require further inquiry.

## CONCLUSIONS

In summary, the synthesis of stereospecifically [<sup>2</sup>H]-labeled **1** enabled us to provide evidence to support that CcTAM catalyzes its isomerization reaction along a path similar to that of TcPAM from a plant. That is, both likely overcome a torsional barrier to access two pivotal rotameric intermediates. CcTAM converts one rotamer to (R)-**2** as the major product through retention of configuration. This pathway competes with a route involving a second rotamer, producing (S)-**2** as the minor enantiomer through inversion of configuration. TcPAM uses only one rotamer to advance to a single enantiomer, (R)- $\beta$ -phenylalanine.

Thus, this study potentially starts to shed light on how CcTAM catalysis uses the 4'-hydroxyl group to orient the substrate in the active site. In addition, this investigation provides a basis by which to probe the driving force that rotates the branch point intermediate in CcTAM to produce two enantiomers.

## MATERIALS AND METHODS

**Chemicals and Reagents.** (S)- $\alpha$ -Tyrosine, 4'-hydroxycinnamic acid, unlabeled- and [<sup>2</sup>H]-4'-hydroxybenzaldehyde, hippuric acid, ethyl chloroformate, (S)-2-methylbutyric anhydride, acetic anhydride, pyridine, bicyclo[2.2.1]hepta-2,5-diene (norbornadiene), <sup>2</sup>H<sub>2</sub> gas, (2S)-[3,3-<sup>2</sup>H<sub>2</sub>]- $\alpha$ -tyrosine ((2S)-[3,3-<sup>2</sup>H<sub>2</sub>]-**1**) and Dowex 50W (100–200 mesh, H<sup>+</sup> form) ion-exchange resin were purchased from Sigma Aldrich (St. Louis, MO). (R)-3-Amino-3-(4'-hydroxyphenyl)propanoic acid and (S)-3-amino-3-(4'-hydroxyphenyl)propanoic acid were purchased from Peptech Inc. (Bedford, MA). (R)-1,2-Bis-(diphenylphosphino)propane ((R)-Prophos) was purchased from Alfa Aesar (Ward Hill, MA). Bicyclo[2.2.1]hepta-2,5-diene-rhodium(I) chloride dimer ([Rh(NBD)Cl]<sub>2</sub>) and silver perchlorate were purchased from Strem Chemicals (Newburyport, MA). Hydrogen gas (99.995% purity) was obtained from Airgas Great Lakes (Independence, OH 44131).

**Instrumentation.** <sup>1</sup>H NMR (500 MHz), <sup>2</sup>H NMR (76.7 MHz) and <sup>13</sup>C NMR (126 MHz) spectra were obtained on a Varian NMR-Spectrometer using standard acquisition parameters. X-ray crystallographic data were collected using a Bruker CCD (charge coupled device)-based diffractometer equipped with an Oxford Cryostream low-temperature apparatus operating at 173 K. The biosynthetic products were quantified and analyzed by gas chromatography/electron-impact mass spectrometry (GC/EIMS): GC (model 6800N, Agilent, Santa Clara, CA) was coupled to a mass analyzer (model 5973 inert, Agilent, Santa Clara, CA) in ion scan mode from 50 to 400 atomic mass units. The GC conditions were as follows: column temperature was held at 200 °C for 1 min and then increased linearly at 20 °C/min to 250 °C with a 1-min hold. Splitless injection was selected, and helium was used as the carrier gas.

**Subcloning, Expression, and Purification of CcTAM.** The *ccTam* cDNA was codon-optimized by GenScript (Piscataway, NJ 08854) in the pUCS7 vector. The clone was ligated into the pET-28a(+) vector between the *Nde*I/*Bam*HI cloning sites. Recombinant plasmids were used to transform *Escherichia coli* BL21(DE3) cells, which were grown in 1 L Luria–Bertani medium supplemented with kanamycin (50  $\mu$ g/mL). Overexpression of CcTAM was induced by the addition of isopropyl- $\beta$ -D-thiogalactopyranoside (100  $\mu$ M) to the

medium, and the cells were grown at 16 °C for 16 h. The cells were then harvested by centrifugation, and the resulting pellet was resuspended in buffer (50 mL of 50 mM sodium phosphate containing 5% (v/v) glycerol, 300 mM NaCl, and 10 mM imidazole, pH 8.0). The cells were lysed by sonication, and the cellular debris and light membranes were removed by centrifugation. The crude, functionally soluble aminomutase was purified by nickel nitrilotriacetic acid (Ni-NTA) affinity chromatography according to the protocol described by the manufacturer (Qiagen, Valencia, CA). Fractions that eluted from the column, containing active CcTAM (62 kDa) in 250 mM imidazole, were combined. The buffer was exchanged with 50 mM sodium phosphate (pH 8.0) containing 5% (v/v) glycerol through several concentration/dilution cycles, using a Centriprep centrifugal filter (30,000 MWCO, Millipore). The purity of the concentrated CcTAM (15 mg/mL in 4 mL, estimated by the Bradford method) was >95% by SDS-PAGE with Coomassie Blue staining.

**Assessing the Activity and Stereochemistry of the CcTAM Reaction.** (S)-**1** (1 mM) was incubated with CcTAM (0.1 mg) at 31 °C in 50 mM phosphate buffer (1 mL, pH 8.5) for 1 h. The assay mixtures were treated in twice (5 min each time) with pyridine (0.6 mmol) and ethyl chloroformate (0.5 mmol). This step, containing excess ethyl chloroformate, caused partial ethyl esterification. Afterward, the reaction was acidified to pH 2 (6 M HCl), and the 4'-O<sub>2</sub>-N- and 4'-O<sub>3</sub>-N-di(ethoxycarbonyl) derivative of  $\alpha$ - and  $\beta$ -tyrosine, respectively, were extracted into ether and treated with a slight excess of diazomethane. The resulting sample contained a mixture of ethyl (~20 mol %) and methyl (80 mol %) esters. 4'-Hydroxycinnamic acid byproduct was converted to its 4'-O-ethoxycarbonyl-(E)-coumaric acid ethyl (10 mol %) and methyl (90 mol %) esters under these conditions. The methyl esters of the  $\alpha$ -tyrosine derivative and the 4'-O-ethoxycarbonyl-(E)-coumaric acid, and the ethyl ester of the  $\beta$ -tyrosine derivative were analyzed by GC/EIMS.

To confirm the stereochemistry of the  $\beta$ -isomer product,<sup>23</sup> another sample of CcTAM (0.1 mg) was incubated at 31 °C with (S)-**1** (1 mM) in phosphate buffer (1 mL, pH 8.5) for 1 h. To this solution were added pyridine (50  $\mu$ L, 0.64 mmol) and (S)-2-methylbutyric anhydride (10  $\mu$ L, 0.05 mmol), and the mixture was stirred vigorously for 5 min. Another batch of pyridine (0.64 mmol) and (S)-2-methylbutyric anhydride (0.05 mmol) was added, and the reaction was stirred for 5 min. The solution was acidified to pH 2 (6 M HCl) and extracted with diethyl ether (3  $\times$  2 mL). The ether fractions were combined and dried. The resulting residue was dissolved in diethyl ether (100  $\mu$ L) and the solution was titrated with a dilute solution of diazomethane dissolved in diethyl ether until the yellow color persisted. These samples were analyzed by GC/EIMS and compared to the retention time and mass fragmentation of authentic standards (See SI).

**Synthesis of Authentic (S)-1, (R)-2, and (E)-4-Hydroxycinnamic Acid Derivatives.** To (S)- $\alpha$ -, (R)- $\beta$ -tyrosine or (E)-4'-hydroxycinnamic acid (0.1 mmol of each) dissolved in 50 mM phosphate buffer (1 mL, pH 8.5) were added pyridine (200  $\mu$ L, 2.4 mmol) and ethyl chloroformate (200  $\mu$ L, 1.6 mmol). The reactions were stirred for 5 min and treated with another batch of pyridine and ethyl chloroformate (both at 200  $\mu$ L) for 5 min with stirring. The ethanolic mixtures caused partial ethyl esterification. Each mixture was acidified to pH 2 (6 M HCl), and extracted into diethyl ether (3  $\times$  2 mL). The ether fractions were combined, dried under vacuum, and the residue was dissolved in methanol (100  $\mu$ L). To this solution was added a dilute diazomethane solution dissolved in diethyl ether, until the yellow color persisted. This procedure resulted in a mixture of ethyl and methyl esters for each sample, as described earlier.

**4'-O-Ethoxycarbonyl-(E)-coumaric Acid Methyl Ester (i.e., 4'-O-Ethylcarboxy-(E)-cinnamic Acid Methyl Ester).** The coumarate ester was recrystallized from ethanol and isolated at 80% yield (20 mg). HRMS: *m/z* 251.0890 ([M + H]<sup>+</sup>); calculated *m/z* 251.0919 ([C<sub>13</sub>H<sub>15</sub>O<sub>5</sub>]<sup>+</sup>). <sup>1</sup>H NMR (500 MHz, CDCl<sub>3</sub>)  $\delta$ : 7.68 (d, *J* = 16.1 Hz, 1 H), 7.55 (d, *J* = 8.3 Hz, 2 H), 7.22 (d, *J* = 8.3 Hz, 1 H), 6.41 (d, *J* = 16.1 Hz, 1 H), 4.34 (q, *J* = 7.3 Hz, 2 H), 3.82 (s, 3 H), 1.41 (t, *J* = 7.3 Hz, 3 H). <sup>13</sup>C NMR (126 MHz, CDCl<sub>3</sub>)  $\delta$ : 167.2 (C(O)OCH<sub>3</sub>), 153.2 (OC(O)O), 152.4 (C4'), 143.6 (C $\beta$ ), 132.2 (C1'), 129.2 (C2'),



121.6 (C3'), 118.1 (C $\alpha$ ), 65.1 (C(O)OCH<sub>3</sub>), 51.7 (OCH<sub>2</sub>CH<sub>3</sub>), 14.2 (OCH<sub>2</sub>CH<sub>3</sub>). (See SI Figures S9–S11 for NMR spectra and GC/EIMS fragmentation data).

**The 4'-O,2-N-Di(ethoxycarbonyl)- $\alpha$ -tyrosine Methyl Ester.** A mixture of ethyl (10 mol %) and methyl (90 mol %) esters of 4'-O,2-N-di(ethoxycarbonyl)- $\alpha$ -tyrosine was obtained at 74% yield (25 mg). The methyl ester of the  $\alpha$ -tyrosine derivative was used in the GC/EIMS analyses of labeled and unlabeled  $\alpha$ -tyrosine substrates. Therefore, the mixed ester sample, dissolved in chloroform (500  $\mu$ L), was loaded onto a preparative silica gel TLC plate and eluted with 90:10 hexane/ethyl acetate. Authentic 4-O,2-N-diethoxycarbonyl- $\alpha$ -tyrosine methyl ester was isolated ( $R_f$  = 0.65) at 67% yield (22.5 mg). HRMS:  $m/z$  419.1781 ([M + H + pyridine]<sup>+</sup>); calculated  $m/z$  419.1818 ([C<sub>21</sub>H<sub>27</sub>N<sub>2</sub>O<sub>7</sub>]<sup>+</sup>). <sup>1</sup>H NMR (500 MHz, CDCl<sub>3</sub>)  $\delta$ : 7.21–6.98 (m, 4 H), 5.10 (d,  $J$  = 7.3 Hz, 1 H), 4.67–4.55 (m, 1 H), 4.28 (q,  $J$  = 7.1 Hz, 2 H), 4.08 (q,  $J$  = 6.7 Hz, 2 H), 3.69 (s, 3 H), 3.10 (dd,  $J$  = 6.1, 14.0 Hz, 1 H), 3.05 (dd,  $J$  = 6.1, 14.0 Hz, 1 H), 1.36 (t,  $J$  = 7.0 Hz, 3 H), 1.20 (t,  $J$  = 6.7 Hz, 3 H). <sup>13</sup>C NMR (126 MHz, CDCl<sub>3</sub>)  $\delta$ : 171.9 (C(O)OCH<sub>3</sub>), 155.8 (OC(O)NH), 153.5 (OC(O)O), 150.2 (C4'), 133.6 (C1'), 130.3 (C2'), 121.0 (C3'), 64.8 (C(O)OCH<sub>3</sub>), 61.2 (CH<sub>2</sub>CH<sub>2</sub>OC(O)NH), 54.5 (CH<sub>2</sub>CH<sub>2</sub>OC(O)O), 52.3 (C $\alpha$ ), 37.6 (C $\beta$ ), 14.4 (CH<sub>2</sub>CH<sub>2</sub>OC(O)NH), 14.1 (CH<sub>2</sub>CH<sub>2</sub>OC(O)O) (See Figures S12–S16 of SI A for NMR spectra and GC/EIMS fragmentation data).

**4'-O,2-N-Di(ethoxycarbonyl)- $\alpha$ -tyrosine Ethyl Ester.** The corresponding ethyl ester was isolated ( $R_f$  = 0.50) from the TLC plate at 7% yield (2.5 mg). HRMS:  $m/z$  433.1933 ([M + H + pyridine]<sup>+</sup>); calculated  $m/z$  433.1974 ([C<sub>22</sub>H<sub>29</sub>N<sub>2</sub>O<sub>7</sub>]<sup>+</sup>). <sup>1</sup>H NMR (500 MHz, CDCl<sub>3</sub>)  $\delta$ : 7.17 (d,  $J$  = 8.6 Hz, 2 H), 7.14–7.11 (m,  $J$  = 8.6 Hz, 2 H), 5.14 (d,  $J$  = 7.8 Hz, 1 H), 4.63 (dd,  $J$  = 5.6, 13.4 Hz, 1 H), 4.33 (q,  $J$  = 7.1 Hz, 2 H), 4.17 (q,  $J$  = 7.2 Hz, 2 H), 4.12 (q,  $J$  = 7.1 Hz, 2 H), 3.11 (d,  $J$  = 5.1 Hz, 2 H), 1.40 (t,  $J$  = 7.1 Hz, 3 H), 1.25 (t,  $J$  = 7.3 Hz, 3 H), 1.24 (t,  $J$  = 7.2 Hz, 3 H). <sup>13</sup>C NMR (126 MHz, CHCl<sub>3</sub>)  $\delta$ : 171.7 (C(O)OCH<sub>3</sub>), 156.1 (OC(O)NH), 153.8 (OC(O)O), 150.4 (C4'), 133.9 (C1'), 130.6 (C2'), 121.3 (C3'), 65.1 (CH<sub>2</sub>CH<sub>2</sub>OC(O)), 61.8 (CH<sub>2</sub>CH<sub>2</sub>OC(O)NH), 61.4 (CH<sub>2</sub>CH<sub>2</sub>OC(O)O), 54.9 (C $\alpha$ ), 38.0 (C $\beta$ ), 14.7 (CH<sub>2</sub>CH<sub>2</sub>OC(O)), 14.4 (CH<sub>2</sub>CH<sub>2</sub>OC(O)NH), 14.3 (CH<sub>2</sub>CH<sub>2</sub>OC(O)O) (See SI Figures S15 and S16 for NMR spectra and GC/EIMS fragmentation data).

**4'-O,3-N-Di(ethoxycarbonyl)- $\beta$ -tyrosine Ethyl Ester.** A mixture of ethyl (33 mol %) and methyl (67 mol %) esters of 4'-O,3-N-diethoxycarbonyl- $\beta$ -tyrosine was isolated ( $R_f$  = 0.38) at 68% yield (24 mg). The ethyl ester of the  $\beta$ -tyrosine derivative was used in the GC/EIMS analyses of labeled and unlabeled biosynthetic  $\beta$ -tyrosines. Thus, authentic ethyl ester was purified by silica gel TLC (90:10 hexane/ethyl acetate). 4'-O,2-N-Di(ethoxycarbonyl)- $\beta$ -tyrosine ethyl ester was isolated at 23% yield (8 mg). HRMS:  $m/z$  433.1922 ([M + H + pyridine]<sup>+</sup>); calculated  $m/z$  433.1974 ([C<sub>22</sub>H<sub>29</sub>N<sub>2</sub>O<sub>7</sub>]<sup>+</sup>). <sup>1</sup>H NMR (500 MHz, CDCl<sub>3</sub>)  $\delta$ : 7.30 (d,  $J$  = 8.8 Hz, 2 H), 7.12 (d,  $J$  = 8.8 Hz, 2 H), 5.67 (d,  $J$  = 6.8 Hz, 1 H), 5.12 (br s, 1 H), 4.28 (q,  $J$  = 7.3 Hz, 2 H), 4.08 (q,  $J$  = 6.8 Hz, 2 H), 4.05 (q,  $J$  = 7.0 Hz, 2 H), 2.91–2.69 (m, 2 H), 1.36 (t,  $J$  = 7.1 Hz, 3 H), 1.20 (t,  $J$  = 6.8 Hz, 3 H), 1.14 (t,  $J$  = 7.3 Hz, 3 H). (See SI Figures S17–S19 for NMR spectra and GC/EIMS fragmentation data). <sup>13</sup>C NMR (126 MHz, CDCl<sub>3</sub>)  $\delta$ : 170.7 (C(O)OCH<sub>2</sub>CH<sub>3</sub>), 155.8 (OC(O)NH), 153.5 (OC(O)O), 150.3 (C4'), 138.8 (C1'), 127.4 (C2'), 121.3 (C3'), 64.8 (CH<sub>2</sub>CH<sub>2</sub>OC(O)), 61.0 (CH<sub>2</sub>CH<sub>2</sub>OC(O)NH), 60.7 (CH<sub>2</sub>CH<sub>2</sub>OC(O)O), 51.0 (C $\beta$ ), 40.6 (C $\alpha$ ), 14.5 (CH<sub>2</sub>CH<sub>2</sub>OC(O)), 14.1 (CH<sub>2</sub>CH<sub>2</sub>OC(O)NH), 14.0 (CH<sub>2</sub>CH<sub>2</sub>OC(O)O).

**4'-O,3-N-Di(ethoxycarbonyl)- $\beta$ -tyrosine Methyl Ester:** isolated ( $R_f$  = 0.54) at 46% yield (16 mg). HRMS:  $m/z$  419.1770 ([M + H + pyridine]<sup>+</sup>); calculated  $m/z$  419.1818 ([C<sub>21</sub>H<sub>27</sub>N<sub>2</sub>O<sub>7</sub>]<sup>+</sup>). <sup>1</sup>H NMR (500 MHz, CDCl<sub>3</sub>)  $\delta$ : 7.29 (d,  $J$  = 8.5 Hz, 2 H), 7.12 (d,  $J$  = 8.5 Hz, 1 H), 5.66 (br s, 1 H), 5.17–5.07 (m, 1 H), 4.28 (q,  $J$  = 6.9 Hz, 2 H), 4.08 (q,  $J$  = 7.3 Hz, 2 H), 3.60 (s, 3 H), 2.90–2.73 (m, 2 H), 1.36 (t,  $J$  = 7.3 Hz, 3 H), 1.20 (t,  $J$  = 7.0 Hz, 3 H). <sup>13</sup>C NMR (126 MHz, CD<sub>3</sub>COCD<sub>3</sub>)  $\delta$ : 170.7 (C(O)OCH<sub>3</sub>), 155.9 (OC(O)NH), 153.4 (OC(O)O), 150.5 (C4'), 140.3 (C1'), 128.4 (C2'), 121.7 (C3'), 65.0 (C(O)OCH<sub>3</sub>), 64.4 (CH<sub>2</sub>CH<sub>2</sub>OC(O)NH), 60.0 (CH<sub>2</sub>CH<sub>2</sub>OC(O)O),

51.0 (C $\beta$ ), 40.2 (C $\alpha$ ), 14.1 (CH<sub>2</sub>CH<sub>2</sub>OC(O)NH), 13.6 (CH<sub>2</sub>CH<sub>2</sub>OC(O)O) (See SI Figures S20–S21 for NMR spectra).

**Synthesis of [Rh(NBD)<sub>2</sub>]ClO<sub>4</sub> Complex.** The [Rh(NBD)<sub>2</sub>]ClO<sub>4</sub> complex was synthesized according to a described process.<sup>35,43</sup> Briefly, a mixture of dimeric [Rh(NBD)Cl]<sub>2</sub> (0.46 g, 1 mmol) and norbornadiene (0.19 g, 2 mmol) dissolved in CH<sub>2</sub>Cl<sub>2</sub> (15 mL) was added to silver perchlorate (0.42 g, 2 mmol) under N<sub>2</sub> and stirred for 1 h. The suspension was filtered to remove the white precipitate, and the filtrate was diluted with dry THF (15 mL). The sample was concentrated under vacuum until the orange needles of [Rh(NBD)<sub>2</sub>]ClO<sub>4</sub> appeared. The crystals were collected, washed with ice-cold, dry THF, and dried under vacuum to obtain 0.65 g (85% isolated yield) of rust brown crystals. <sup>1</sup>H NMR (500 MHz, CDCl<sub>3</sub>)  $\delta$ : 5.20 (q,  $J$  = 2.0 Hz, 4 H), 4.13 (br s, 2 H), 1.51 (t,  $J$  = 1.6 Hz, 2 H).

**Synthesis of [Rh(NBD)((R)-Prophos]ClO<sub>4</sub> Complex.** The Rh-Prophos catalyst was prepared by an established procedure.<sup>35,43</sup> To the orange-red solution of [Rh(NBD)<sub>2</sub>]ClO<sub>4</sub> (0.54 g, 1.4 mmol) and (R)-Prophos (0.57 g, 1.4 mmol) dissolved in a mixture of dry CH<sub>2</sub>Cl<sub>2</sub> and THF (5 mL of each) was added hexane (5 mL) dropwise under N<sub>2</sub>. The solution stood, undisturbed at room temperature for 5 h, and then at 5 °C for 16 h. Orange-red crystals were collected by vacuum filtration and washed with ice-cold, dry THF and then with hexane. The crystals were dried under N<sub>2</sub> to obtain 0.8 g (80% isolated yield) of the Rh-catalyst. <sup>1</sup>H NMR (500 MHz, CDCl<sub>3</sub>)  $\delta$ : 7.79–7.73 (m, 2 H), 7.72–7.67 (m, 3 H), 7.65–7.61 (m, 2 H), 7.61–7.58 (m, 6 H), 7.58–7.55 (m, 6 H), 7.47–7.41 (m, 2 H), 7.35–7.29 (m, 2 H), 5.42 (br s, 2 H), 5.33 (br s, 1 H), 5.31 (s, 1 H), 4.87 (br s, 1 H), 4.28 (br s, 1 H), 4.16 (br s, 1 H), 3.84–3.67 (m, 1 H), 2.71–2.59 (m, 2 H), 2.57 (d,  $J$  = 2.2 Hz, 1 H), 2.04 (td,  $J$  = 7.4, 12.9 Hz, 1 H), 1.88–1.84 (m, 1 H), 1.84–1.76 (m, 2 H), 1.20 (dd,  $J$  = 6.5, 12.3 Hz, 4 H). <sup>13</sup>C NMR (126 MHz, DMSO-*d*<sub>6</sub>)  $\delta$ : 143.1, 135.1, 135.1, 134.8, 134.5, 134.1, 133.9, 132.8, 132.7, 132.0, 131.9, 131.7, 131.1, 131.0, 130.9, 130.1, 129.3, 129.3, 128.9, 128.8, 128.8, 128.6, 128.5, 128.2, 127.8, 125.9, 125.5, 67.0, 63.4, 48.2, 25.1, 14.8, 14.6.

**Synthesis of [<sup>2</sup>H]-Labeled (2S)-1 Isotopomers.** *Synthesis of (Z)-2-Benzamido-3-(4'-hydroxyphenyl)acrylic Acid.* According to a described procedure,<sup>44</sup> a mixture of 4-hydroxybenzaldehyde (1.9 g, 12.5 mmol), K<sub>2</sub>HPO<sub>4</sub> (2.2 g, 12.5 mmol), and acetic anhydride (3.8 mL, 40 mmol) was stirred and heated at 80 °C under N<sub>2</sub> for 5 min. To the mixture was added hippuric acid (2.3 g, 12.5 mmol) in one lot, and the reaction was stirred at 80 °C for 2 h. Yellow crystals were collected by vacuum filtration and washed with water to obtain an oxazolone intermediate (3.1 g, 81% yield) that was used without further purification. To the oxazolone (3.07 g, 10 mmol) was added 2% NaOH in 70% aqueous ethanol (100 mL), and the suspension was refluxed for 12 h. The reaction mixture was cooled to room temperature, diluted with distilled water (~50 mL) and titrated with 12 M HCl until precipitation of the product ceased. The mixture was vacuum filtered, washed with distilled water, dried, and recrystallized from ethanol/water (70:30, v/v) to obtain 3 g (85% yield) of the desired product. <sup>1</sup>H NMR (500 MHz, DMSO-*d*<sub>6</sub>)  $\delta$ : 12.49 (br s, 1 H), 9.91 (s, 1 H), 9.77 (s, 1 H), 7.99 (d,  $J$  = 7.1 Hz, 2 H), 7.59 (t,  $J$  = 7.3 Hz, 1 H), 7.54 (dd,  $J$  = 3.4, 8.8 Hz, 3 H), 7.51 (d,  $J$  = 7.3 Hz, 1 H), 6.77 (d,  $J$  = 8.7 Hz, 2 H), <sup>13</sup>C NMR (126 MHz, DMSO-*d*<sub>6</sub>)  $\delta$ : 166.6, 165.9, 158.8, 134.0, 133.7, 131.9, 131.8, 128.5, 128.3, 127.7, 127.5, 124.6, 124.0, 115.5, 115.4. See SI for crystallographic data.

*Synthesis of (Z)-2-Benzamido-[3-<sup>2</sup>H]-3-(4'-hydroxyphenyl)acrylic Acid.* The [<sup>3-<sup>2</sup>H</sup>]-acrylic acid isotopomer was synthesized analogously to the unlabeled isomer (above), except [<sup>2-<sup>2</sup>H</sup>]-4'-Hydroxybenzaldehyde (0.62 g, 5 mmol) was used. Acetic anhydride (1.6 mL, 17 mmol), K<sub>2</sub>HPO<sub>4</sub> (0.9 g, 5 mmol), and hippuric acid (0.9 g, 5 mmol) were varied to make the intermediate oxazolone (1.26 g, 82% yield). The oxazolone (1.23 g, 4 mmol) was saponified under reflux with ethanolic NaOH as before. The mixture was diluted with distilled water (25 mL), and the product was precipitated by the adding 12 M HCl at room temperature. The suspension was worked up and the product was recrystallized as described previously to obtain 1 g (88% yield) of product. <sup>1</sup>H NMR (500 MHz, DMSO-*d*<sub>6</sub>)  $\delta$ : 12.49 (s, 1 H), 9.91 (s, 1 H), 9.77 (s, 1 H), 7.99 (d,  $J$  = 7.1 Hz, 1 H), 7.60 (t,  $J$  = 7.3 Hz, 1 H), 7.56–7.48 (m, 4 H), 6.77 (d,  $J$  = 8.8 Hz, 1 H). <sup>13</sup>C NMR (126 MHz,

DMSO- $d_6$ )  $\delta$ : 166.6, 165.9, 158.8, 133.8, 131.9, 131.8, 131.6, 128.5, 128.4, 127.7, 127.5, 124.6, 123.9, 115.6, 115.4. See SI for crystallographic data.

**Synthesis of (2S,3S)-[2,3- $^2$ H $_2$ ]- and (2S,3R)-[3- $^2$ H]-1.** The following procedure is based on previously described methods.<sup>35,43,45</sup> (Z)-2-Benzamido-[3- $^2$ H]-3-(4'-hydroxyphenyl) acrylic acid (1 g, 3.5 mmol) and 10 mg of [Rh(NBD)((R)-Prophos)]ClO<sub>4</sub> were dissolved in dry THF (25 mL) in a Parr reactor. The reactor was successively evacuated and filled with H<sub>2</sub> gas and kept under H<sub>2</sub> gas (2.0 bar) for 16 h. The solvent was evaporated, followed by azeotropic removal of residual THF with methanol. To the resultant yellow residue dissolved in methanol (15 mL) was added dry Dowex 50 W (100–200 mesh) cation exchange resin (1.5 g). The mixture was stirred until a clear solution was obtained, and then filtered. The retained resin was washed with warm methanol. All methanol filtrates were combined and dried under vacuum to obtain the crude *N*-benzoyl-(2S,3R)-[3- $^2$ H]-tyrosine (0.9 g). The product was then refluxed with 40% HBr (aqueous) (10 mL) for 3 h. The mixture was cooled to room temperature, and the benzoic acid crystals were removed by filtration. The filtrate was washed with diethyl ether (3  $\times$  20 mL) to remove residual benzoic acid. The aqueous layer was lyophilized, and the crude product was dissolved in 0.2 M NaOH (10 mL) and acidified with acetic acid to yield crystals after 1 h at 0 °C. The product was isolated by vacuum filtration and the retentate was washed with ice cold water to yield (2S,3R)-[3- $^2$ H]-1 as its zwitterionic amino acid (0.41 g, 70% yield).

(2S,3S)-[2,3- $^2$ H $_2$ ]-1 was synthesized by a procedure analogous to that described for the synthesis of (2S,3R)-[3- $^2$ H]-1 with the following exceptions. (Z)-2-Benzamido-3-(4'-hydroxyphenyl)acrylic acid was used instead of the unlabeled isotopomer, and D<sub>2</sub> gas was used in place of H<sub>2</sub> gas for the reduction step to obtain (2S,3S)-[2,3- $^2$ H $_2$ ]-1 as the zwitterionic amino acid (0.38 g, 65% yield).

**Characterization of (2S,3S)-[2,3- $^2$ H $_2$ ]- and (2S,3R)-[3- $^2$ H]-1.** (2S,3S)-[2,3- $^2$ H $_2$ ]- and (2S,3R)-[3- $^2$ H]-1 (1  $\mu$ mol of each) were separately derivatized to their 4'-O,*N*-di(ethoxycarbonyl) derivatives in water (1 mL) with ethyl chloroformate (50  $\mu$ L, 0.5 mmol) and pyridine (50  $\mu$ L, 0.6 mmol), and the samples were acidified to pH 2 (6 M HCl) and extracted into diethyl ether (1 mL). After treatment of the ethanolic extract with diazomethane, the derivatives were isolated as a mixture of ethyl (10 mol %) and methyl (90 mol %) esters, as described before. The methyl-esterified amino acid derivative was analyzed by GC/EIMS. The [ $^2$ H]-labeled fragment ions originating from the identically derivatized (2S)-[3,3- $^2$ H $_2$ ]-1 were used to interpret the structures of various ions. The relative ratio of diagnostic [ $^2$ H]-labeled ions was compared to that of identical fragment ions of the unlabeled (S)-1 derivative to calculate the deuterium enrichment of labeled isotopomers: (2S,3S)-[2,3- $^2$ H $_2$ ]-1 and (2S,3R)-[3- $^2$ H]-1 (Table S1 and Figures S21–S24 of SI).

The coupling constants (*J*) for the geminal protons (H<sub>A</sub> and H<sub>B</sub>) against H<sub>X</sub> observed by <sup>1</sup>H NMR for authentic (S)-1 in D<sub>2</sub>O were *J*<sub>AX</sub> = 5.0 Hz at  $\delta$  3.23 (H<sub>A</sub>) and *J*<sub>BX</sub> = 7.8 Hz at  $\delta$  3.08 (H<sub>B</sub>). In a previous study, the preferred conformation of (S)-1 in water was established by NMR using stereospecifically deuterium isotopomers of 1 to correlate chemical shift and the magnitude of coupling constants with the conformation of the prochiral hydrogens.<sup>36</sup> These earlier findings put the dihedral angle between the carboxy group and the aromatic ring at 180°. In this conformation, H<sub>A</sub> and H<sub>X</sub> were separated by ~60°, and H<sub>B</sub> and H<sub>X</sub> by 180°. Using this earlier data along with the magnitude of the *J* values<sup>36</sup> observed for (S)-1, we assigned H<sub>A</sub> as *pro*-(3S) and H<sub>B</sub> as *pro*-(3R). This data was used to assign the absolute stereochemistry at C <sub>$\beta$</sub>  of the synthetic (2S,3S)-[2,3- $^2$ H $_2$ ]- and (2S,3R)-[3- $^2$ H]-1.

Authentic (S)-1 (10 mg) was dissolved in D<sub>2</sub>O (1 mL), and transferred to a 5 mm diameter NMR tube, and analyzed by <sup>1</sup>H NMR [(500 MHz, D<sub>2</sub>O, 32 scans, 25 °C)  $\delta$ : 7.23 (d, *J* = 8.5 Hz, 2 H), 6.93 (d, *J* = 8.5 Hz, 2 H), 3.97 (dd, *J* = 5.1, 7.8 Hz, 1 H), 3.23 (dd, *J* = 5.0, 14.7 Hz, 1 H), 3.08 (dd, *J* = 7.8, 14.7 Hz, 1 H)]. (2S,3S)-[2,3- $^2$ H $_2$ ]- and (2S,3R)-[3- $^2$ H]-1 (10 mg of each) were separately dissolved in D<sub>2</sub>O (and H<sub>2</sub>O) and analyzed by <sup>1</sup>H NMR (and <sup>2</sup>H NMR). (2S,3S)-[2,3- $^2$ H $_2$ ]-1: <sup>1</sup>H NMR (500 MHz, D<sub>2</sub>O, 32 scans, 25 °C)  $\delta$ : 7.23 (d, *J*

= 8.5 Hz, 2 H), 6.93 (d, *J* = 8.5 Hz, 2 H), 3.07 (s, 1 H). <sup>2</sup>H NMR (77 MHz, H<sub>2</sub>O, 512 scans, 25 °C)  $\delta$ : 3.97 (bs, 1 H), 3.21 (bs, 1 H). (2S,3R)-[3- $^2$ H]-1: <sup>1</sup>H NMR (500 MHz, D<sub>2</sub>O, 32 scans, 25 °C)  $\delta$ : 7.23 (d, *J* = 8.3 Hz, 2 H), 6.93 (d, *J* = 8.8 Hz, 2 H), 3.97 (d, *J* = 4.9 Hz, 1 H), 3.22 (d, *J* = 4.9 Hz, 1 H). <sup>2</sup>H NMR (77 MHz, H<sub>2</sub>O, 512 scans, 25 °C)  $\delta$ : 3.07 (bs, 1 H) (Figure S25 of SI).

**Synthesis of Authentic 4'-O,3-*N*-di((S)-2-Methylbutanoyl) Methyl Esters of (R)- and (S)-2.** To a sample of (R)- and (S)-2 (0.5  $\mu$ mol of each) dissolved in 50 mM phosphate buffer (1 mL) were added pyridine (50  $\mu$ L, 0.6 mmol) and (S)-2-methylbutyric anhydride (10  $\mu$ L, 5  $\mu$ mol) at 0 °C. The reactions were stirred for 5 min and treated with another batch of pyridine (50  $\mu$ L) and (S)-2-methylbutyric anhydride (10  $\mu$ L) and stirred for 5 min. The mixtures were each acidified (pH 2 with 6 M HCl) and extracted with diethyl ether (3  $\times$  2 mL). The ether fractions were combined, dried under vacuum, and the residue was dissolved in methanol (100  $\mu$ L). To this solution was added a dilute diazomethane solution dissolved in diethyl ether, until the yellow color persisted. The resultant 4'-O,3-*N*-di((S)-2-methylbutanoyl)- $\beta$ -tyrosine methyl ester diastereoisomers were analyzed by GC/EIMS; their retention times and fragment ions are noted in SI Figure S26.

**Assessing the Stereospecificity of the C <sub>$\beta$</sub> -Hydrogen Abstraction Catalyzed by CcTAM.** (2S,3S)-[2,3- $^2$ H $_2$ ]- and (2S,3R)-[3- $^2$ H]-1 (each at 1 mM) were separately incubated with CcTAM (0.1 mg) at 31 °C in 50 mM phosphate buffer (1 mL, pH 8.5) for 1 h. The tyrosine isomers were derivatized *in situ* with ethyl chloroformate (50  $\mu$ L, 0.5 mmol) and pyridine (50  $\mu$ L, 0.6 mmol) to their 4'-O,*N*-di(ethoxycarbonyl) derivatives. The samples were acidified to pH 2 (6 M HCl) and extracted into diethyl ether (1 mL). After treatment of the ethanolic extract with excess diazomethane, the amino acid derivatives were isolated as a mixture of ethyl and methyl esters and analyzed by GC/EIMS, as before. Diagnostic fragment ions from the ethyl ester derivative of the biosynthetic  $\beta$ -2 were analyzed to determine the regiochemistry of the deuterium atoms.

**Assessing the Stereospecificity of the Hydrogen Rebound at C <sub>$\alpha$</sub>  Catalyzed by CcTAM.** (2S)-[3,3- $^2$ H $_2$ ]-1 (5 mM) was incubated with CcTAM (0.8 mg) at 31 °C in 50 mM phosphate buffer (40 mL, pH 8.5) for 36 h. The incubation mixture was lyophilized, and the remaining residue was dissolved in methanol (7 mL) for <sup>2</sup>H NMR analysis or CD<sub>3</sub>OD (7 mL) for <sup>1</sup>H NMR analysis. As a control sample, authentic unlabeled (R)-2 (2 mM) in 50 mM phosphate buffer (40 mL, pH 8.5) was lyophilized, and the remaining residue was dissolved in CD<sub>3</sub>OD (7 mL) for <sup>1</sup>H NMR analysis. The magnitude of the coupling constants of the ABX spin system observed in the <sup>1</sup>H NMR for authentic unlabeled (R)-2 in CD<sub>3</sub>OD was used to assign the chemical shifts of the protons at the prochiral center of 2. This data was then used to assign the absolute stereochemistry at C <sub>$\alpha$</sub>  of the biosynthetic [ $^2$ H]-2.

**Assessing the Intramolecular Proton Transfer Step of the CcTAM Reaction.** (2S)-[3,3- $^2$ H $_2$ ]-1 (1 mM) was incubated with CcTAM (0.1 mg) at 31 °C in 50 mM phosphate buffer (10 mL, pH 8.5). Aliquots (1 mL) were withdrawn from the reaction mixture at 10 min, then at 2, 4, 7, 12, 22, 33, and 45 h. The samples were derivatized *in situ* with ethyl chloroformate (50  $\mu$ L, 0.5 mmol) and pyridine (50  $\mu$ L, 0.6 mmol) to their 4'-O,*N*-di(ethoxycarbonyl) derivatives, acidified to pH 2 (6 M HCl), and extracted into diethyl ether (1 mL). After treatment of the ethanolic extract with diazomethane, the amino acid derivatives were isolated as a mixture of ethyl and methyl esters. During the derivatization, 4'-hydroxycinnamate was converted to its 4'-O-ethoxycarbonyl-(*E*)-coumaric acid as an ethyl and methyl ester mixture. The methyl esters of the  $\alpha$ -tyrosine and (*E*)-coumaric acid derivatives and the ethyl ester of the  $\beta$ -tyrosine derivative were analyzed by GC/EIMS (see SI Figures S6 and S7 for representative diagnostic fragment ions observed for the derivatized biosynthetic 2 and 4'-hydroxycinnamate in this time course study). GC/EIMS was used in selected-ion mode to calculate the ion abundance ratio of [ $^2$ H]<sub>1</sub>(M)<sup>+</sup> (*m/z* 354) and [ $^2$ H]<sub>2</sub>(M)<sup>+</sup> (*m/z* 355) for the derivatives of the biosynthetic deuterium labeled 2. This ratio informed on the D  $\rightarrow$  H exchange during the reaction. The ion abundance of [ $^2$ H]<sub>2</sub>(M)<sup>+</sup> (*m/z* 355) was corrected by subtracting the abundance of the naturally



occurring  $^{13}\text{C}$ -isotopomer (i.e., the  $[\text{H}_1](M+1)^+$  ( $m/z$  355) of the molecular ion  $[\text{H}_1](M)^+$  ( $m/z$  354)) of the singly deuterium-labeled derivative.

**Assessing the Effect of pH on CcTAM Stereoselectivity.** (S)-1 (1 mM) was incubated with CcTAM (0.1 mg) separately at pHs 7, 8, and 9 (6 mL of each) in 50 mM phosphate buffer at 31 °C. Aliquots (1 mL) were withdrawn at 1, 2.5, 5, 11, and 25 h. The amino acids were derivatized *in situ* with (S)-2-methylbutyric anhydride to form the 4'-O,3-N-di((S)-2-methylbutanoyl)-2 and methyl esterified with diazomethane and analyzed by GC/EIMS. The sum of ion abundances for fragment ions  $m/z$  278  $[\text{M} - \text{methyl butyl}]^+$  (90% of base peak) and  $m/z$  194  $[\text{M} - (2 \times \text{methyl butyl}) + \text{H}]^+$  (base peak) for each enantiomer was compared to calculate the ratio of (R)- and (S)-2 in the sample.

**Synthesis of (R)-2 Methyl Ester.** In brief, to (R)-2 (18.1 mg, 0.1 mmol) dissolved in methanol (1 mL, 25 mmol) was added trimethylsilyl chloride (25  $\mu\text{L}$ , 0.2 mmol).<sup>46</sup> The suspension was stirred for 16 h and the methanol was evaporated *in vacuo* to obtain the product (19.5 mg, quantitative yield).  $^1\text{H}$  NMR (500 MHz,  $\text{CD}_3\text{OD}$ )  $\delta$ : 7.29 (d, 8.5 Hz, 2 H), 6.85 (d, 8.5 Hz, 2 H), 4.63 (dd,  $J = 6.3, 7.8$  Hz, 1 H), 3.69 (s, 3 H), 3.09 (dd,  $J = 7.8, 17.0$  Hz, 1 H), 2.98 (dd,  $J = 6.3, 17.0$  Hz, 1 H).

## ■ ASSOCIATED CONTENT

### ● Supporting Information

Gas chromatography and mass spectrometry data, NMR data, D  $\rightarrow$  H exchange plot, and CIF data. This material is available free of charge via the Internet at <http://pubs.acs.org>.

## ■ AUTHOR INFORMATION

### Corresponding Author

walker@chemistry.msu.edu

### Notes

The authors declare no competing financial interest.

## ■ ACKNOWLEDGMENTS

This material is based on work supported by NSF-CAREER Award 0746432. We thank Dr. Richard Staples (Center for Crystallographic Research, Michigan State University) for providing the X-ray crystallographic data. The high-resolution mass spectrometry was done by Dr. Gavin Reid at Michigan State University, Department of Chemistry.

## ■ REFERENCES

- (1) Ahn, H. J.; Kim, Y. S.; Kim, J.-U.; Han, S. M.; Shin, J. W.; Yang, H. O. *J. Cell. Biochem.* **2004**, *91*, 1043–1052.
- (2) Garcion, E.; Lamprecht, A.; Heurtault, B.; Paillard, A.; Aubert-Pouessel, A.; Denizot, B.; Menei, P.; Benoit, J. P. *Mol. Cancer Ther.* **2006**, *5*, 1710–1722.
- (3) Belyaev, N. A.; Kolesanova, E. F.; Kelesheva, L. F.; Rotanova, T. V.; Panchenko, L. F. *Bull. Exp. Biol. Med.* **1990**, *110*, 1483–1485.
- (4) Prabhakaran, P. C.; Woo, N. T.; Yorgey, P. S.; Gould, S. J. *J. Am. Chem. Soc.* **1988**, *110*, 5785–5791.
- (5) Liu, W.; Christenson, S. D.; Standage, S.; Shen, B. *Science* **2002**, *297*, 1170–1173.
- (6) Yin, X. H.; O'Hare, T.; Gould, S. J.; Zabriskie, T. M. *Gene* **2003**, *312*, 215–224.
- (7) Rachid, S.; Krug, D.; Weissman, K. J.; Müller, R. *J. Biol. Chem.* **2007**, *282*, 21810–21817.
- (8) Weaver, D. F.; Tan, C. Y. K.; Kim, S. T.; Kong, X.; Wei, L.; Carran, J. R. (Queen's University at Kingston, Canada; Neurochem Inc.). Antiepileptogenic agents. Patent WO/2002/073208, March 13, 2002.
- (9) Georg, G. I. *The Organic Chemistry of  $\beta$ -Lactams*; Wiley-VCH: New York, 1993.

- (10) Gademann, K.; Kimmerlin, T.; Hoyer, D.; Seebach, D. *J. Med. Chem.* **2001**, *44*, 2460–2468.
- (11) Sonti, R.; Gopi, H. N.; Muddegowda, U.; Ragothama, S.; Balaran, P. *Chem.—Eur. J.* **2013**, *19*, 5955–5965.
- (12) Murray, J. K.; Farooqi, B.; Sadowsky, J. D.; Scalf, M.; Freund, W. A.; Smith, L. M.; Chen, J.; Gellman, S. H. *J. Am. Chem. Soc.* **2005**, *127*, 13271–13280.
- (13) Ibrahim, I.; Rios, R.; Vesely, J.; Zhao, G.-L.; Cordova, A. *Synthesis* **2008**, 1153–1157.
- (14) Davies, S. G.; Mulvaney, A. W.; Russell, A. J.; Smith, A. D. *Tetrahedron: Asymmetry* **2007**, *18*, 1554–1566.
- (15) Tan, C. Y. K.; Weaver, D. F. *Tetrahedron* **2002**, *58*, 7449–7461.
- (16) Chesters, C.; Wilding, M.; Goodall, M.; Micklefield, J. *Angew. Chem., Int. Ed.* **2012**, *51*, 4344–4348.
- (17) Ratnayake, N. D.; Wanninayake, U.; Geiger, J. H.; Walker, K. D. *J. Am. Chem. Soc.* **2011**, *133*, 8531–8533.
- (18) Magarvey, N. A.; Fortin, P. D.; Thomas, P. M.; Kelleher, N. L.; Walsh, C. T. *ACS Chem. Biol.* **2008**, *3*, 542–554.
- (19) Mutatu, W.; Klettke, K. L.; Foster, C.; Walker, K. D. *Biochemistry* **2007**, *46*, 9785–9794.
- (20) Walker, K. D.; Klettke, K.; Akiyama, T.; Croteau, R. *J. Biol. Chem.* **2004**, *279*, 53947–53954.
- (21) Christianson, C. V.; Montavon, T. J.; Festin, G. M.; Cooke, H. A.; Shen, B.; Bruner, S. D. *J. Am. Chem. Soc.* **2007**, *129*, 15744–15745.
- (22) Christianson, C. V.; Montavon, T. J.; Van Lanen, S. G.; Shen, B.; Bruner, S. D. *Biochemistry* **2007**, *46*, 7205–7214.
- (23) Krug, D.; Müller, R. *ChemBioChem* **2009**, *10*, 741–750.
- (24) Rother, D.; Poppe, L.; Viergutz, S.; Langer, B.; Retey, J. *Eur. J. Biochem.* **2001**, *268*, 6011–6019.
- (25) Asano, Y.; Kato, Y.; Levy, C.; Baker, P.; Rice, D. *Biotransform.* **2004**, *22*, 131–138.
- (26) Rettig, M.; Sigrist, A.; Rétey, J. *Helv. Chim. Acta* **2000**, *83*, 2246–2265.
- (27) Montavon, T. J.; Christianson, C. V.; Festin, G. M.; Shen, B.; Bruner, S. D. *Bioorg. Med. Chem. Lett.* **2008**, *18*, 3099–3102.
- (28) Feng, L.; Wanninayake, U.; Strom, S.; Geiger, J.; Walker, K. D. *Biochemistry* **2011**, *50*, 2919–2930.
- (29) Strom, S.; Wanninayake, U.; Ratnayake, N. D.; Walker, K. D.; Geiger, J. H. *Angew. Chem., Int. Ed.* **2012**, *51*, 11–17.
- (30) Christenson, S. D.; Wu, W.; Spies, M. A.; Shen, B.; Toney, M. D. *Biochemistry* **2003**, *42*, 12708–12718.
- (31) Sasse, F.; Kunze, B.; Gronewold, T. M. A.; Reichenbach, H. *J. Natl. Cancer Inst.* **1998**, *90*, 1559–1563.
- (32) Lambert, J. B.; Shurvell, H. F.; Lightner, D.; Cooks, R. G. *Organic Structural Spectroscopy*; 1st ed.; Prentice Hall: NJ, 1998.
- (33) Jensen, F. R.; Bushweller, C. H. *J. Am. Chem. Soc.* **1969**, *91*, 3223–3225.
- (34) Garbisch, E. W.; Griffith, M. G. *J. Am. Chem. Soc.* **1968**, *90*, 6543–6544.
- (35) Fryzuk, M. D.; Bosnich, B. *J. Am. Chem. Soc.* **1978**, *100*, 5491–5494.
- (36) Oba, M.; Ueno, R.; Fukuoka, M.; Kainosho, M.; Nishiyama, K. *J. Chem. Soc., Perkin Trans. 1* **1995**, 1603–1609.
- (37) Kumar, S.; Dwevedi, A.; Kayastha, A. M. *J. Mol. Catal. B: Enzym.* **2009**, *58*, 138–145.
- (38) Stingl, K.; Uhlemann, E. M.; Schmid, R.; Altendorf, K.; Bakker, E. P. *J. Bacteriol.* **2002**, *184*, 3053–3060.
- (39) Cooke, H. A.; Bruner, S. D. *Biopolymers* **2010**, *93*, 802–810.
- (40) Katz, B. A.; Elrod, K.; Verner, E.; Mackman, R. L.; Luong, C.; Shrader, W. D.; Sendzik, M.; Spencer, J. R.; Sprengeler, P. A.; Kolesnikov, A.; Tai, V. W. F.; Hui, H. C.; Breitenbucher, J. G.; Allen, D.; Janc, J. W. *J. Mol. Biol.* **2003**, *329*, 93–120.
- (41) Hanoian, P.; Sigala, P. A.; Herschlag, D.; Hammes-Schiffer, S. *Biochemistry* **2010**, *49*, 10339–10348.
- (42) Lyubimov, A. Y.; Lario, P. I.; Moustafa, I.; Vrieliink, A. *Nat. Chem. Biol.* **2006**, *2*, 259–264.
- (43) Fryzuk, M. D.; Bosnich, B. *J. Am. Chem. Soc.* **1977**, *99*, 6262–6267.



- (44) Cleary, T.; Brice, J.; Kennedy, N.; Chavez, F. *Tetrahedron Lett.* **2010**, *51*, 625–628.
- (45) Kirby, G. W.; Michael, J. J. *Chem. Soc., Perkin Trans. 1* **1973**, 115–120.
- (46) Li, J.; Sha, Y. *Molecules* **2008**, *13*, 1111–1119.